Inorganic Chemistry © Cite This: Inorg. Chem. 2019, 58, 16642–16659

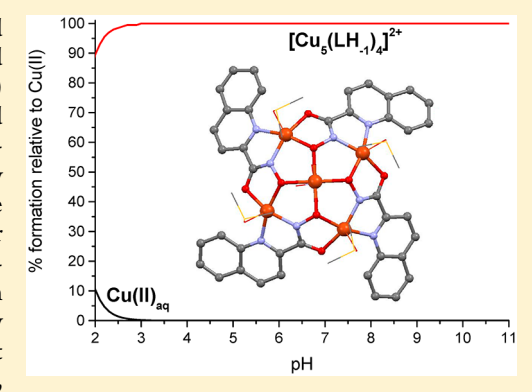
pubs.acs.org/IC

Explaining How α -Hydroxamate Ligands Control the Formation of Cu(II)-, Ni(II)-, and Zn(II)-Containing Metallacrowns

Malgorzata Ostrowska,[†] Yuliya Toporivska,[†] Irina A. Golenya,[‡] Sergiu Shova,[∥] Igor O. Fritsky,[‡] Vincent L. Pecoraro, and Elzbieta Gumienna-Kontecka*, but a control of the contro

Supporting Information

ABSTRACT: Four different crystal structures for quinolinehydroxamic acid (QuinHA) and picolinehydroxamic acid (PicHA) MCs with Cu(II) and Ni(II), and solution studies on the formation of Cu(II), Ni(II), and Zn(II) MC complexes with QuinHA, PicHA, and pyrazylohydroxamic acid (PyzHA) are described. In polynuclear complex 1, [Cu₅(QuinHA-2H)₄(NO₃)(DMSO)₄](NO₃), the metallamacrocyclic cavity is formed by four Cu(II) ions and four doubly deprotonated hydroximate ligands, and the center of the cavity is occupied by the fifth Cu(II) ion coordinated by four hydroximate oxygen atoms. The complex 2, [Cu10(PicHA-2H)₈(H₂O)₄(ClO₄)₃](ClO₄)·4H₂O, exhibits a dimeric structure based on two pentanuclear collapsed 12-MC-4 Cu₄(PicHA-2H)₄ fragments united by two chiral capping Cu(II) ions exo-coordinated to the peripheral vacant (O,O') chelating units of each tetranuclear collapsed MC moiety. 3, $[CaNi_5(QuinHA-2H)_5(H_2O)_2(Py)_{10}](NO_3)_2$, and 4, $[CaNi_5(PicHA-2H)_5(H_2O)_2(Py)_{10}](NO_3)_2$



2H)₅(DMF)₂(Py)₈](NO₃)₂, are planar 15-membered rings consisting of a PicHA or QuinHA ligand, respectively. To understand fully the correlation between species isolated in the solid state and those presented in solution, the solution equilibria were investigated, showing the dependence of the MCs topologies and stability constants (log β) on the ligand structure and metal ion.

■ INTRODUCTION

In recent years, there has been significant growth in research interest in transition metal coordination compounds of high nuclearity. These molecules possess very interesting properties allowing for their use as active components of molecular materials, new sources for luminescent or second harmonic generation (SHG) materials, and the core of functional metalorganic frameworks (MOFs) or large coordination polymers. 1-8 Among the earliest identified self-assembled polynuclear complexes based on transition metal-ligand building blocks, metallacrowns (MCs) have attracted considerable attention. $^{9-11}$

MCs are cyclic metal/organic compounds, which are considered as crown ether analogs in their structure and function. The scaffold of MCs is conceptually obtained by replacing the methylene carbons of crown ethers with metalheteroatom coordination units. As with crown ethers, they are characterized by the presence of an oxygen rich core cavity, which may encapsulate guest species. 10,12,13 Due to their capacity to bind cations of almost any group-alkali, alkaline earth and transition metals, lanthanides, and main group metals and metalloids—as well as anions or neutral molecules, they have been recognized to be relevant compounds in a variety of research fields. Metallacrowns have been reported as single-molecule magnets (SMMs) and potential precursors for qubits, 14-19 magnetorefrigerants, 20,21 MOFs, cation and anion recognition agents, 22-25 and luminescent probes. 26-31 Establishing the solution stability of MCs, their selectivity for metal ions, and their guest recognition properties is essential for the design of functional compounds and materials based on MCs scaffolds. Therefore, more detailed characterization of the thermodynamic parameters associated with the assembly of MCs would be useful. This is particularly necessary in order to predict whether new MC-forming ligands that have been conceived to optimize magnetic or photophysical properties that will serve as building blocks for desired MC scaffolds. Optimization of ligands includes the development of chelators that have a high stability across a broad pH range.

One of the versatile ligand classes capable of forming polynuclear complexes, including MCs, are hydroxamic acids. MCs structure can be obtained by self-assembly of a proper

Received: September 12, 2019 Published: November 21, 2019



[†]Faculty of Chemistry, University of Wroclaw, 50-383 Wroclaw, Poland

[‡]Department of Chemistry, Taras Shevchenko National University of Kyiv, 64 Volodymyrska Str., 01601 Kiev, Ukraine

[§]Department of Chemistry, University of Michigan, Ann Arbor, Michigan 48109, United States

 $^{^{\}parallel st}$ Poni Petru" Institute of Macromolecular Chemistry, Aleea Gr. Ghica Voda 41A, 700487 Iasi, Romania

Scheme 1. Schematic Representation of the Ligands Used in This Study

number of the coordination units of hydroxamic acids, functionalized in the α , β , or γ position with respect to the hydroximate function, and metal ions. ^{9,32,33} Following the *metallacrown structural paradigm*, hydroximate ligands with additional donor function in β -position, preferably assemble into 12-MC-4, while α -hydroximate derivatives prefer the formation of 15-MC-5 complexes. ^{10,33} However, in the past few years exceptions to the MC structural paradigm have been reported. It has been shown that α -aminohydroximates are able to form thermodynamically stable 12-MC-4 with Cu(II) ions. ³³ Formation of both 12-MC-4 and 15-MC-5 complexes of Ni(II) ions with α - and β -aminohydroxamic acids, specifically α -alaninehydroxamic acid (α -AlaHA), β -alaninehydroxamic acid (β -AlaHA), and valinehydroxamic acid (ValHA), has also been observed. ^{34,35}

One of the MC-forming ligands most extensively described in the literature, 22,27,36-44 both in solution and in the solid state, is o-picolinehydroxamic acid (PicHA). Inspired by the results obtained for PicHA, we decided to extend the studies to other aromatic hydroxamate derivatives that have recently been used to prepare extremely bright, near-IR-emissive MCs. 26,27,30,31 In this paper we describe four different crystal structures for quinolinehydroxamic acid (QuinHA) and PicHA MCs with Cu(II) and Ni(II) and present solution studies on the formation of Cu(II), Ni(II), and Zn(II) MC complexes with QuinHA, PicHA, and pyrazylohydroxamic acid (PyzHA), Scheme 1. A comparison of the thermodynamic stabilities of Cu(II), Ni(II), and Zn(II) MC species with the studied ligands reveal that by the modification of the ligand structure, one can tune the pH range of MC self-assembly and the thermodynamic stability of the complexes. The results presented here allow us to understand better the influence of the ligand structure (aromaticity, bulkiness), as well as subtle factors such as axial ligands (symmetricity of disposition vs MC plane, denticity, size, etc.) and solvation effects, on the formation and stability of MC species in solution and solid

■ EXPERIMENTAL SECTION

Reagents. All reagents were commercial products of reagent grade (Sigma-Aldrich or POCH) and were used without further purification. **Caution!** Although no problems were encountered in this work, transition metal perchlorate complexes are potentially explosive and should be handled with proper precautions.

Synthesis and Crystallization. *Ligands Synthesis.* Quinolinehydroxamic, picolinehydroxamic, and pyrazylohydroxamic acids were synthesized and purified as previously reported. ^{27,40}

Crystallization of $[Cu_5(QuinHA-2H)_4(NO_3)(DMSO)_4](NO_3)$ (1, $\{Cu-(II)[12-MC_{Cu/(II),QuinHA}-4]^{2+}\}$. In a 25 mL Erlenmeyer flask $Cu(NO_3)_2$. $3H_2O$ (24 mg, 0.1 mmol), **QuinHA** (18 mg, 0.1 mmol), and 2 equiv of KOH (11.2 mg, 0.2 mmol) were combined together and stirred in 8 mL of MeOH/DMSO solution (70/30 w/w) for 2 h, resulting in

the precipitation of a green microcrystals. DMSO (3 mL) was added, and the solution was heated up to 60 °C for 2 h. The suspension was filtered, and the homogeneous solution was transferred into a glass vial, which was placed in a wide-mouth jar containing diethyl ether. Dark green crystals suitable for X-ray analysis were obtained after 2 days. The crystals were isolated by filtration, rinsed with cold water, and air-dried. Yield 20%. Elemental analysis for $C_{40}H_{24}N_8O_8Cu_5$ calcd: C, 45.33; H, 2.88; N,10.58; found: C, 45.03; C, 49.1; C, 10.64. C, 45.1 C, 46.1 C, 47.1 C, 47.1 C, 47.1 C, 48.1 C, 49.1 C,

Crystallization of $[Cu_{10}(PicHA-2H)_8(H_2O)_4(ClO_4)_3](ClO_4)\cdot 4H_2O$ (2, collapsed $[Cu_{10}(PicHA-2H)_8(H_2O)_4(ClO_4)_3]^+)$. The solution of Cu(ClO₄)₂·6H₂O in EtOH (27 mg, 0.1 mmol, 5 mL) was added to solution of **PicHA** in EtOH (13.8 mg, 0.1 mmol, 5 mL). To the obtained mixture, thiourea dissolved in EtOH (1.3 mg, 0.016 mmol, 1 mL) was added, and the transparent green solution was left for crystallization by slow diffusion with diethyl ether vapors in a closed vessel at room temperature. Dark-green needle-shaped crystals suitable for X-ray analysis were obtained after 48–72 h. They were filtered, washed with diethyl ether, and air-dried. Yield: 77%. Elemental analysis: for $Cu_{10}C_{48}H_{48}N_{16}O_{40}Cl_4$ (2266.25) calcd: C, 25.44; H, 2.14; N, 9.89; found: C, 25.66; H, 1.98; N, 9.95.

Crystallization of [CaNi₅(QuinHA-2H)₅(H₂O)₂(Py)₁₀](NO₃)₂ (3, {Ca(II)[15-MC_{Ni(II),QuinHA}-5]]²⁺. Ni(C₂H₃O)₂·4H₂O (24.8 mg, 0.1 mmol), and QuinHA (18.9 mg, 0.1 mmol) were mixed in 5 mL of MeOH for 5 h, followed by an addition of Ca(NO₃)₂ (0.05 mmol, 8.2 mg) in MeOH (3 mL); the solution was left for slow evaporation at room temperature until dark yellow powder appeared. The solid was collected by filtration, air-dried, and dissolved in 5 mL of pyridine/DMF mixture (50/50 w/w). The solution obtained was filtered, and the filtrate was set to crystallize by ethyl acetate vapor diffusion. Yellowish crystals suitable for X-ray analysis were obtained after 3 days. The crystals were isolated by filtration, rinsed with cold water, and air-dried. Yield 25%. Elemental analysis for C₅₀H₃₅N₁₀O₁₀Ni₅Ca calcd: C, 47.62; H, 2.79; N, 10.85; found: C, 48.03; H, 3.09; N, 10.84. ESI-MS (MeOH) m/z 631.92 {Ni₅(QuinHA)₅Ca}²⁺.

Crystallization of [CaNi₅(PicHA-2H)₅(DMF)₂(Py)₈](NO₃)₂ (4, {Ca-(II)[15-MC_{Ni(II),PicHA}-5])²⁺). Ni(C₂H₃O)₂·4H₂O (24.8 mg, 0.1 mmol), PicHA (27.6 mg, 0.2 mmol), Ca(NO₃)₂ (0.025 mmol, 4.1 mg), and NaOH (20 mg, 0.5 mmol) were combined together and dissolved in 10 mL of MeOH. A yellow solution obtained was stirred for 1 h and left for slow evaporation at room temperature. An acquired gel was dissolved in 5 mL of pyridine/DMF mixture (50/50 w/w). The solution was filtered and left for slow diffusion with ethyl acetate. Yellowish crystals suitable for X-ray analysis were obtained after 3 days. The crystals were isolated by filtration, rinsed with cold water, and air-dried. Yield 26%. Elemental analysis for C₃₀H₂₀N₁₀O₁₀Ni₅Ca calcd: C, 35.68; H, 1.99; N, 13.86; found: C, 35.54; H, 2.09; N, 13.95. ESI-MS (methanol) m/z 505.89 {(Ni₅(PicHA)₅Ca)²⁺.

Crystallization of [Ni(PicHA-H)₂(Py)₂]·(Py) (5, {Ni(II)(PicHA-H)₂}). Ni(NO₃)₂·6H₂O (29 mg, 0.1 mmol), and PicHA (27.6 mg, 0.2 mmol) were mixed in 6 mL of MeOH. Two mL of pyridine was added dropwise, and stirring was continued for 30 min. The transparent yellow solution was subjected to slow diffusion with tert-butyl methyl ether in a closed vessel under ambient conditions. Brown single crystals suitable for X-ray analysis obtained within 24–48 h were filtered, rinsed with methanol, and air-dried. Yield 71%.

Elemental analysis for $NiC_{27}H_{25}N_7O_4$ (570.23) calcd: C 56.87, H 4.42, N 17.19; found: C 57.05, H 4.52, N 17.00.

X-ray Crystal Structure Determination. Single-crystal X-ray crystallographic data for 1, 3, and 4 were collected at 193(2) K, on a Xcalibur Ruby CCD-based X-ray diffractometer with graphite-monochromatic Mo– K_{α} radiation (λ = 0.71073 Å) using the ω -scan technique. Intensity data for 2 were collected with Oxford Diffraction SuperNova diffractometer using hi-flux micro-focus Nova Cu K α radiation (λ = 1.54184 Å), while for 5 were carried out with an Oxford-Diffraction XCALIBUR E CCD diffractometer equipped with graphite-monochromated Mo K α radiation.

The unit cell determination and data integration were carried out using the CrysAlis package of Oxford Diffraction. ⁴⁵ The structures were solved by direct methods using $Olex2^{46}$ software with the SHELXT structure solution program and refined by full-matrix least-squares on F^2 with SHELXL-2015. ⁴⁷ The hydrogen atoms attached to carbon were placed in fixed, idealized positions ($d_{CH} = 0.96 \text{ Å}$) and refined as rigidly bonded to the corresponding non-hydrogen atoms. O–H hydrogen atoms were located from the difference Fourier map and verified by corresponding H-bonds parameters. CCDC 1952100 for 1, 1952101 for 2, 1952102 for 3, 1952103 for 4, and 1952104 for 5 contain the supplementary crystallographic data for this contribution. These data can be obtained free of charge via www.ccdc.cam.ac.uk/conts/retrieving.html (or from the Cambridge Crystallographic Data Centre, 12 Union Road, Cambridge CB2 1EZ, UK; fax: (+44) 1223-336-033; or deposit@ccdc.ca.ac.uk).

- 1: The methyl groups of the DMSO molecule were found to be disordered over two positions with occupancies of 0.623 and 0.377, respectively. Two oxygen atoms of the coordinated nitrate ion and all four atoms of the non-coordinated nitrate ion were found to be disordered over two positions with equal occupancies. The N-O bond lengths involving these nitrate ions were restrained to ensure proper geometry using DFIX instruction of SHELXL. ⁴⁰ To achieve reasonable anisotropic displacement ellipsoids, a further EADP instruction was applied for the disordered atoms of both DMSO methyl groups and the nitrate ions.
- 2: The crystals were weakly diffracting; the resolution has been estimated at 0.95 Å. Four oxygen atoms of three perchlorate anions and two oxygen atoms of one perchlorate anion were found to be disordered over two positions with occupancies of 0.5. Several solvate water molecules were found to be disordered as well, having occupancies of 0.5 or 0.33. The positional parameters of disordered ClO₄⁻ counteranions and water molecules were refined using available tools (PART, DFIX, and SADI) of SHELXL-2015, and the combined anisotropic/isotropic refinement has been applied for non-hydrogen atoms.
- 3: One nitrate ion, two coordinated water molecules as well as several solvate water molecules were found to be disordered over two positions with equal occupancies. The N–O bond lengths involving the disordered nitrate ion were restrained to ensure proper geometry using SADI instruction of SHELXL. To achieve reasonable anisotropic displacement ellipsoids, a further EADP instruction was applied for the disordered atoms of the disordered nitrate ion. Two solvate pyridine molecules were found to be disordered with solvate water molecules with occupancy factors of 0.75 for pyridine and 0.25 for water molecules.
- 4: Three-coordinated pyridine rings were found to be disordered over two positions, two of them with equal occupancies and one with the occupancy factors 0.665/0.335. One solvate DMF molecule was found to be disordered over two positions with equal occupancies, the thermal parameters of the non-hydrogen atoms of this molecule were refined isotropically. To achieve reasonable geometric and anisotropic displacement parameters, further SADI, EADP, and ISOR instructions of SHELXL⁴⁰ were applied for the disordered atoms of the pyridine rings and DMF molecule.

Potentiometric Titrations. The potentiometric titrations were carried out in a MeOH/ H_2O (80:20 w/w) mixture or H_2O (PyzHA was the only ligand for which speciation studies could be carried out by us in water). The ionic strength was adjusted to 0.1 M with the addition of NaCl. Carbonate-free standardized NaOH solution was used (H_2O) or prepared by dissolution of NaOH in deoxygenated MeOH/ H_2O (80:20 w/w) mixture, and was standardized using potassium hydrogen phthalate. HCl solution was titrated by standardized NaOH solution. Zn(II), Ni(II), and Cu(II) stock solutions were standardized by ICP-AES along with the complexometric titration with standardized Na $_2H_2$ EDTA and murexide (CuCl $_2$ and NiCl $_2$) and xylenol orange (ZnCl $_2$).

For all titrations, an automatic titrator system Titrando 905 (Metrohm), connected to a combined glass electrode (Mettler Toledo InLab Semi-Micro) filled with 0.1 M NaCl in a MeOH/H₂O (80:20 w/w) mixture (Mettler Toledo InLab Semi-Micro), was used. The electrode was calibrated daily in terms of hydrogen ion concentration by titrating HCl solution. As stream of CO₂- and O₂-free argon was used during titrations. All the titrations were carried out in a pH range 2–11, on 3 mL samples with the ligand concentration of ca. 3×10^{-3} M and metal-to-ligand molar ratios 1:2 and 1:3. The exact concentration of the ligands was calculated using the method of Gran. The potentiometric data were processed using the Superquad 49 and Hyperquad 2006 programs, which base on nonlinear least-squares methods. The ionic product of water, pK_w, in the MeOH/H₂O (80:20 w/w) mixture was $10^{-14.42}$ mol 2 dm $^{-6.52}$

UV-Vis Spectrophotometry. Absorption spectra were recorded on a Varian Cary 300 Bio or a Varian Cary 50 UV-vis spectrophotometer, using Hellma quartz optical cells with 1 or 5 cm path length. Sample solutions had compositions similar to those employed in potentiometry. The initial pH of solutions was adjusted to around 2, and then the titrations were carried out by the addition of small volumes of NaOH. Data were processed using Origin 7.0 or Specfit programs.

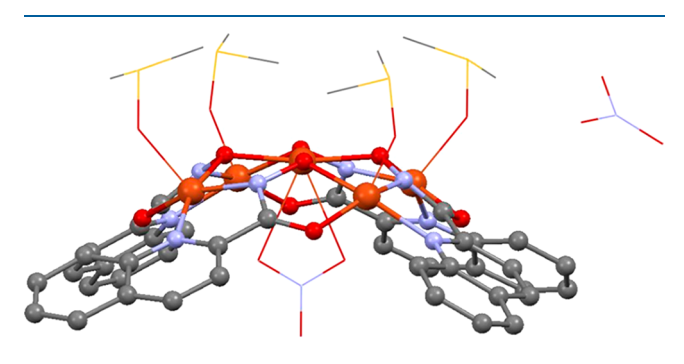
EPR Spectroscopy. Electron paramagnetic resonance spectra were recorded in liquid nitrogen on a Bruker ELEXSYS E500 CW-EPR spectrometer equipped with an NMR teslameter (ER 036TM) and frequency counter (E 41 FC) at X-band frequency. The ligand concentration was 3×10^{-3} M, and metal-to-ligand molar ratio was 1:3. The solutions for EPR were prepared with addition of 30% of ethylene glycol as a cryoprotectant. The spectra were recorded in the pH range from 1 to 10.5. The pH of samples was adjusted to expected by use of appropriate volumes of HCl and NaOH solutions. The experimental spectra were simulated using WINEPR Simfonia 1.26 program and Spin (EPR of S > 1/2) program by Dr. Andrew Ozarowski, National High Field Magnetic Laboratory, University of Florida.

ESI-MS. Electrospray ionization mass spectrometry (ESI-MS) data were recorded on a Bruker Q-FTMS or a Bruker MicrO-TOF-Q (Bruker Daltonik, Bremen, Germany) spectrometers, equipped with an Apollo II electrospray ionization source with an ion funnel. The instrumental parameters of Bruker Q-FTMS were: scan range, m/z 400–1600; dry gas, nitrogen; temperature, 170 °C; capillary voltage, 4500 V; ion energy, 5 eV. The capillary voltage was optimized to the highest signal-to-noise ratio. Parameters of Bruker MicrO-TOF-Q were as follows: scan range, m/z 250–2000; dry gas, nitrogen; temperature, 200 °C; ion source voltage, 4500 V; collision energy, 10 eV. The spectra were recorded in the positive ion mode. MeOH/H₂O solution was used to prepare solutions of ligand with concentrations of 10^{-4} – 10^{-5} M and metal-to-ligand molar ratios 1:1, 1:2, and 1:3.

RESULTS

Structural Description. Cu(II) Metallacrowns. $[Cu_5(QuinHA-2H)_4(NO_3)(DMSO)_4](NO_3)$ (1), are dark green crystals, which were obtained from DMSO solution by slow diffusion with diethyl ether. The compound was obtained in a tetragonal crystal system, space group P4/n. The structure consists of pentanuclear complex monocations exhibiting a 12-

MC-4 topology, with a bound nitrate ion, and an outer-sphere nitrate counterion providing charge balance. The complex cation possesses intrinsic C4 symmetry with a 4-fold rotation axis passing through the central Cu(II) ion, the nitrate nitrogen and one of the nitrate oxygen atoms, while two other nitrate oxygens are disordered over two positions. The metallamacrocyclic cavity is formed by four Cu(II) ions and four doubly deprotonated hydroximate ligands. The center of the cavity is occupied by the fifth Cu(II) ion coordinated by four hydroximate oxygen atoms ($Cu-O_{oxime} = 1.958(5)$ Å). As ligands forming fused 5-membered chelate rings prefer the planar pentagonal topology found in 15-MC-5-type MCs, the complex is highly strained in order to close a cyclic system comprising from 12 fused 5-membered rings. This strain coupled with the square-pyramidal preference for the ring Cu(II) leads to significant distortion from planarity, resulting in a bowl-shaped MC conformation. Unlike PicHA-containing 12-MC-4, ⁴² QuinHA 12-MC-4 structure, 1 is not collapsed, probably due to the presence of an additional aromatic ring in the ligand, which results in stabilization of 12-MC-4 structure and its significant deviation from planarity (Figure 1).



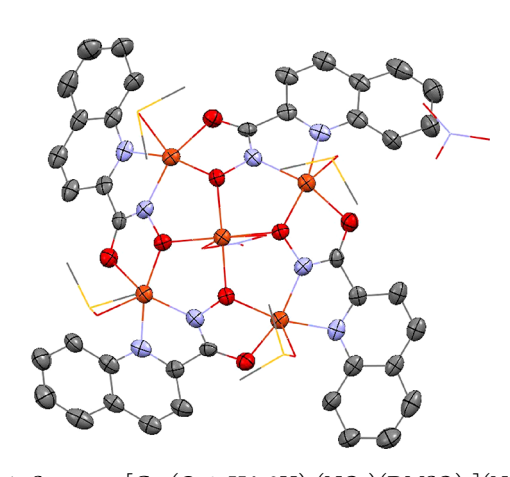


Figure 1. Structure $[Cu_5(QuinHA-2H)_4(NO_3)(DMSO)_4](NO_3)$, 1. Color scheme: orange = Cu, red = O, dark blue = N, gray = C. Lattice solvent molecules and hydrogen atoms were removed; axial ligands are displayed as thin lines in the ball and stick diagram for clarity.

To evaluate the coordination geometry of central ions we used SHAPE 2.1 software ⁵⁴ (Table S7) Each Cu(II) ion of the MC ring has a distorted square pyramidal coordination geometry ($\tau_s = 0.129$), ⁵⁵ with the Cu(II) ions in the equatorial plane coordinated by two oxygen atoms of one **QuinHA** anion and then two nitrogen atoms of a second **QuinHA** anion. Continuing this pattern around the structure leads to the cyclic

sequence based on the M–N–O–M linkage. The Cu– $O_{carbonyl}$ and Cu– O_{oxime} distances are 1.969(6) and 1.970(6) Å, respectively, Cu– N_{imine} is 1.937(6) Å, while Cu– $N_{quinoline}$ is longer than Cu– N_{imine} and equal 2.043(6) Å (Table S2), which is normal for MC complexes. The central Cu(II) is in a distorted square-planar environment formed by four regularly disposed symmetrically related oximino oxygen atoms, while Cu(II) ion is protruded from the basal plane by 0.141(5) Å.

The disposition of the axial ligands linked to the central and ring Cu(II) ions are different with respect to the faces of MC moiety. On the convex face of the MC ring, four DMSO oxygen atoms are bound to ring Cu(II) ions, while on the opposite, concave face of the MC, two oxygen atoms of the chelating nitrate anion are bound to the central Cu(II), complementing its surrounding to hexa-coordinated (severely distorted trigonal-prismatic, as evidenced by SHAPE 2.1 geometry analysis⁵⁴). The apical Cu—O contacts are noticeably longer than the equatorial ones, with a distance of 2.218(6) Å for DMSO molecules, and 2.218(6) for nitrate oxygen atoms ion.

The X-ray structure of 1 is the third of the $\{M(II)[12-MC_{M(II),QuinHA}-4]\}^{2+}$ complexes. The first two 12-MC-4 compounds containing two fused 5-membered ring ligands were formed with Ni(II) and Zn(II) (Table 1).⁴⁰ The cup

Table 1. Structural Parameters for Selected $\{M(II)[12-MC_{M(II),QuinHA}-4]\}^{2+}$ Complexes with QuinHA and Ni(II), Cu(II), and Zn(II)^a

	Ni(II)	Cu(II)	Zn(II)
M _{ring} coord. no.	6	5	5
av M _{ring} -O _{hydroxamate} (Å)	1.995	1.969(6)	2.068
av M _{ring} -O _{carbonyl} (Å)	2.175	1.967(4)	2.006
av M _{ring} -N _{hydroxamate} (Å)	2.023	1.938(6)	2.021
av M_{ring} – $N_{(Py)}$ (Å)	2.16(4)	2.044(6)	2.16(3)
av M_{ring} -O/ $N_{solvent}$ (Å)	2.160	2.74(1)	2.162
av M _{ring} -M _{ring} (Å)	4.813	4.571(1)	4.822
$M-OMP_{MC}^{b}$	0.380(54)	0.300(3)	0.682(161)
av central M-O _{hydroxamate} (Å)	1.965	1.958(5)	2.041
central M-OMP _{MC} ^b	0.39	0.14(2)	0.38
central M coord. no.	5	6	5
central M ionic radius (Å)	0.63	0.65	0.68
central cavity radius ^c	0.57	0.60	0.65

 $^a\{\rm Ni(II)[12\text{-}MC_{\rm Ni(II),QuinHA}\text{-}4]\}^{2+}$ and $\{\rm Zn(II)[12\text{-}MC_{\rm Zn(II),QuinHA}\text{-}4]^{2+}$ from ref 40. Oxygen mean plane for the atoms in the central cavity. $^c\rm Cavity$ radius is calculated as the average distance from the oxygen atom to the centroid of the hydroxamate oxygen atoms minus the ionic radius of an oxygen atom (1.36 Å). 40

shape geometry of 1, with Cu(II) ions in the ring resting far above the equatorial ligand plane was predicted by Tegoni et al. for {Cu(II)[12-MC_{Cu(II), α -aminoHA}-4]}. Shape The depth of the concave face of 1 is 4.26 Å, and its diameter is about 17.8 Å. These parameters are quite close to those observed for {Cu(II)[12-MC_{Cu(II),QuinHA}-4]}^2+ (4.8 and 18.7 Å, respectively) but indicate less pronounced concavity of Cu(II) 12-MC-4. Also, the depth of the concave face is much greater than in the case of Ni(II) 12-MC-4 (1.29 Å), the most planar in the series of QuinHA-containing 12-MC-4. The central cavity radius of 1 is 0.60 Å which fits well to the ionic radius of pentacoordinated Cu(II) (0.65 Å), but still smaller, so that the central Cu(II) ion rests only slightly above the oxygen mean plane (OMP) by 0.142(5) Å which is much less than in the

case of Ni(II) and Zn(II) complexes (0.38-0.39 Å). However, 1 is much more concave than the Ni(II) complex and close to that of the Zn(II) MC by its shape. This is achieved by noticeably shorter M_{ring} - M_{ring} separations (4.571(1) vs 4.82-4.83 Å in Ni(II) and Zn(II) complexes) which compensates for the effect of small displacement of central Cu(II) ion from OMP. In other words, in the case of the Cu(II) MC its cup is blunter than in Ni(II) and Zn(II) MCs. In contrast, the ring Cu(II) ions are removed from the mean planes of their equatorial donor atoms (N2O2) by 0.300(3) Å. The cavity radius is smaller than that of Zn(II) 12-MC-4 complex (0.65 Å), and larger than QuinHA MC Ni(II) analog (0.57 Å) which correlates with the values of ionic radii of the three metal ions (Table 1). The crystal structure of 1 has distortions from planarity intermediate between those of the Ni(II) and Zn(II) (Table 1, Figure 2), exactly as predicted, which provides direct experimental confirmation for the systematic bowling of the $\{M(II)[12-MC_{M(II),\alpha-aminoHA}-4]\}$ topology.

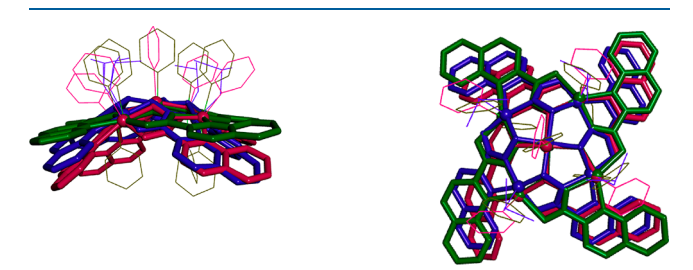


Figure 2. Structural overlay of $\{Ni(II)[12\text{-MC}_{Ni(II),QuinHA^{-4}}]\}^{2+}$ (green), $\{Cu(II)[12\text{-MC}_{Cu(II),QuinHA^{-4}}]\}^{2+}$, 1 (dark blue), and $\{Zn(II)[12\text{-MC}_{Zn(II),QuinHA^{-4}}]\}^{2+}$. The structures are tethered at the four hydroxamate oxygen atoms. Axial ligands are displayed as thin lines in the ball and stick diagram for clarity.

The most interesting observation in comparison of these three structures is the marked difference between the degree of concavity of their MC frameworks. On one hand, Zn(II) and Ni(II) complexes indicate very close geometrical parameters (such as average M_{ring} –N/O bond distances and M_{ring} ··· M_{ring} separations, M_{cent} ···OMP distances); however, they exhibit different degrees of concavity. On the other hand, Zn(II) and

Cu(II) complexes are very similar by their shapes but differ noticeably in geometrical parameters (Cu(II) complex exhibits significantly shorter M_{ring} -N/O and M_{cent} -O distances and M_{ring}...M_{ring} separations). Evidently, in the present case the most planar conformation of Ni(II)-containing complex is conditioned by the octahedral geometry of ring Ni(II) ions having axial pyridine molecules on both sides of MC. As a consequence, the equatorial planes of the Ni(II) ring ions are significantly more planar than in the case of the squarepyramidal Zn(II) and Cu(II). If we apply τ_5 parameter ⁴⁷ for the equatorial planes of the ring Ni(II) ion to estimate the degree of their inclination from the planarity, we receive the values in the range 0.008-0.027, while in the case of Zn(II) and Cu(II) ring metals $\tau_5 = 0.04 - 0.30$ (av. 0.188) and 0.129, respectively. Thus, nearly planar equatorial spheres of Ni(II) ions constituting the 12-MC-4 circuit, bring about the overall essentially more planar overall conformation of the metallamacrocycle. This is reached by the expense of significant loosening the outer $O_{carbonyl}$ – Ni^{II} – $N_{quinHA-pyridyl}$ angles until the values of 120.60–123.59° (for regular octahedron, a 90° is expected) while in Zn(II) and Cu(II) MCs these angles are only 98.69-102.85 and 103.23°, respectively. More concave shape of the Ni(II) complex would lead to unfavorable steric interactions between the neighboring axial pyridine molecules. It is believed that the tetragonal-pyramidal coordination of the central Ni(II), not typical for this ion, is forced, as addition of another axial ligand on the concave face would result in significant steric tension between the pyridine rings. In the cases when the ring metals exhibit pentacoordinated squarepyramidal geometry (Cu(II), Zn(II)) typical for these ions, the MCs adopt a convex conformation with the axial Py ligands disposed on the convex side of MCs due to the presence of unequal number of axial ligands on two sides of the equatorial plane.

Earlier it was demonstrated that disposition of axial ligands in coordination spheres of both ring and central metals can play an important role in realization of specific conformations of MCs. ^{39,57} Such effects have been observed for the Cu(II) 15-MC-5 with different central ions (Ln(III), Pb(II), Hg(II)) indicating a concave conformation. ^{39,57} On the other hand,

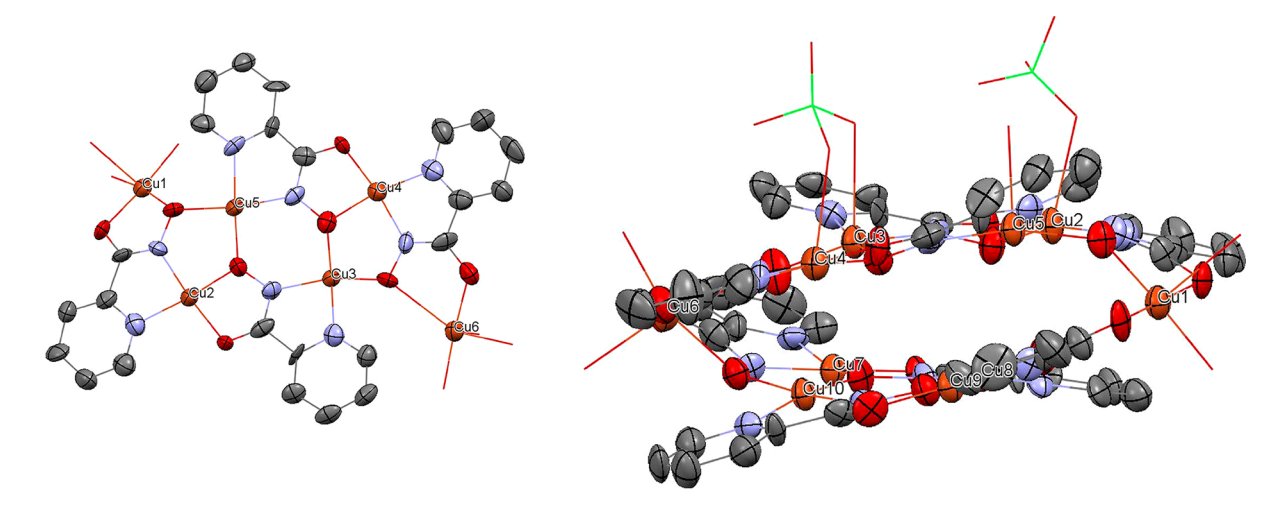


Figure 3. Structure of collapsed MC fragment with two exo-coordinated Cu(II) ions in $[Cu_{10}(PicHA-2H)_8(H_2O)_4(ClO_4)_3](ClO_4)\cdot 4H_2O$, 2 (top), and molecular structure of decanuclear complex $[Cu_{10}(PicHA-2H)_8(H_2O)_4(ClO_4)_3](ClO_4)\cdot 4H_2O$, 2 (bottom). Color scheme: orange = Cu, red = Cu, dark blue = Cu, gray = Cu, light green = Cu. Lattice solvent molecules and hydrogen atoms were removed; axial ligands are displayed as thin lines in the ball and stick diagram for clarity.

analogous complexes having Ni(II) as a ring metal with the same central metals, exhibited nearly planar conformations, as the ring Ni(II) ions indicated typical for them octahedral geometry with equal distribution of axially coordinated Py molecules between two sides of the MC plane.

This example demonstrates again a crucial influence of axial ligands on MC conformation. Uniform and/or symmetric disposition of axial ligands with respect to the MC plane facilitates its more planar conformation. Opposite, asymmetric or unilateral disposition of the axial ligands forces declinations from planarity and thus enhances degree of concavity of the MC framework.

In our earlier work we demonstrated that attempts to obtain [12-MC_{Cu(II),PicHA}-4] in DMSO, DMF, and MeOH resulted in degradation of the 12-MC-4 accompanied by the formation of tetranuclear collapsed MCs [Cu₄(PicHA-H)₂(PicHA-2H)₂]²⁺ or their aggregates. Here, based on an attempt to synthesize the 12-MC-4 from EtOH, with consequent crystallization of the product by slow vapor diffusion of Et₂O, allowed us to isolate a 1D-coordination polymer featuring decanuclear units of composition [Cu₁₀(PicHA-2H)₈(H₂O)₄(ClO₄)₃](ClO₄)· 4H₂O, 2.

The compound crystallizes in triclinic system, the space group $P\overline{1}$. The structure is ionic and consists of singly charged decanuclear complex cations [$Cu_{10}(PicHA-2H)_8(H_2O)_4(ClO_4)_3$]⁺, perchlorate anions, and solvate water molecules. The complex cation, however, exhibits a dimeric structure that is not based on a pentanuclear 12-MC-4 but rather from two collapsed MC $Cu_4(PicHA-2H)_4$ fragments united by two chiral capping Cu(II) ions exo-coordinated to the peripheral vacant (O,O') chelating units of each tetranuclear collapsed MC moiety (Figure 3). A similar exochelation of a fifth Cu(II) ion to the collapsed MC moiety has been observed in 28-nuclear double-stranded metallahelicate based on L-norvaline hydroxamate.⁵⁸

The overall conformation of the decanuclear unit can be described as a double-decked aggregate incorporating two collapsed MC layers, which are linked with two side crosspieces (Figure 3). Notably, each collapsed MC moiety exhibits not a planar, but markedly twisted conformation of a "canted blade". The dihedral angles between the two halves of the "blades" are $25.13(9)^{\circ}$ for the twist around Cu(2)Cu(3)/ Cu(4)/Cu(5) and $24.91(8)^{\circ}$ for Cu(7)Cu(8)/Cu(9)Cu(10). This feature significantly differentiates the present structure from those observed earlier in PicHA-containing Cu(II) collapsed MCs, in which essentially planar conformations of the molecules are observed. 42 This difference is also reflected in a significantly twisted conformation of the central sixmembered bimetallic ring of each collapsed MC deck. The twist angles are 29.18° for the ring Cu(3)N(3)O(3)Cu(5)-O(7)N(7) and 13.87° for Cu(8)N(55)O(11)Cu(10)O(15)-N(15).

Two collapsed MC decks are united by long axial contacts Cu(5)-O(13)=2.8633(2), Cu(10)-O(5)=2.7919(2), and Cu(8)-O(3)=2.9038(2) Å with μ_3 -bridging functions of the hydroxamate oxygen atoms O(13), O(5), and O(3). The fourth similar interdeck contact $Cu(3)\cdots O(11)=3.2637(2)$ is too long to be considered as a coordination axial bond.

Most of Cu(II) ions belonging to the collapsed MC fragments have one or two axial ligands complementing the coordination number to 5 (square pyramidal) or 6 (distorted-octahedral) as calculated using SHAPE 2.1 geometry analysis⁵⁴ (Table S7). Only Cu(9) exhibits a distorted square-planar

geometry with shortened Cu–O and Cu–N distances, as compared to the other Cu(II) ions. The pentacoordinated Cu(II) atoms exhibit different degrees of distortion from a regular tetragonal-pyramidal geometry (τ_5 for Cu(2) = 0.231, Cu(3) = 0.218, Cu(4) = 0.086, Cu(7) = 0.187, Cu(8) = 0.016). The Cu–O axial contact are in the range 2.4902(2) – 2.7721(2) Å for perchlorates and 2.3123(2) Å for water oxygen.

Both "peripheral" Cu(II) ions Cu(1) and Cu(6) are in the pseudo-octahedral environment. Their coordination spheres are formed by six oxygen atoms, with four of them belonging to the outer (O,O') chelating units of two different collapsed MC decks. The two remaining *cis*-situated coordination sites are occupied by water molecules (in the case of Cu(6)) or by water molecule and the carbonyl oxygen atom O(1) of the translational molecule (Cu(1)). Such *cis*-bis(chelate) coordination of Cu(1) and Cu(6) gives rise to configuration chirality of both centers, in the basic decanuclear unit both of them indicate the Δ absolute stereochemical configuration. For both Cu(II) ions, their coordination spheres are severely distorted.

Organization of the decanuclear subunits into 1D-coordination polymeric chains proceed as follows. First, two chiral decanuclear subunits form a centrosymmetric dimer due to two long axial contacts Cu(7)-O(12)(carbonyl) at 2.7274(2) Å. Next, a similar axial interaction of the "peripheral" Cu(1) ions between the centrosymmetrically related the bis-(decanuclear) dimers unite them into a 1D-polymeric motif (Cu(1)-O(1)(carbonyl)) at 2.5623(2) Å) (Figure 4).

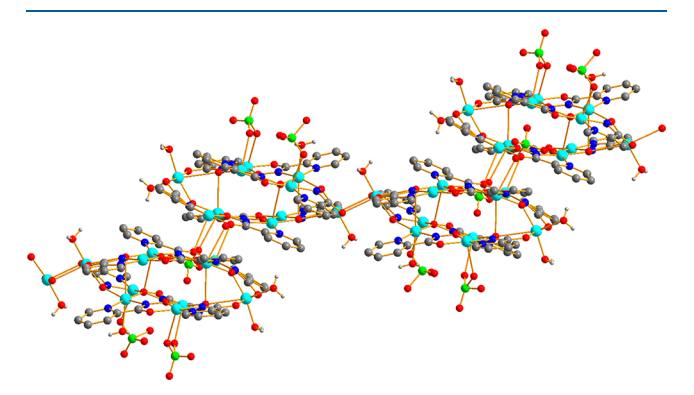


Figure 4. Structure of 1D-polymeric motif of $[Cu_{10}(PicHA-2H)_8(H_2O)_4(ClO_4)_3](ClO_4)\cdot 4H_2O$, **2.** Color scheme: cyan = Cu, red = O, dark blue = N, gray = C, light green = Cl.

Ni(II) Metallacrowns. Several attempts have been made to crystallize the pentanuclear 15-MC-5 complexes of **QuinHA** and **PicHA**. The $[CaNi_5(QuinHA-2H)_5(H_2O)_2(Py)_{10}]-(NO_3)_2$, 3 and $[CaNi_5(PicHA-2H)_5(DMF)_2(Py)_8](NO_3)_2$, 4 were obtained from a pyridine/DMF solution and crystallized by slow diffusion with ethyl acetate (Figure 5). The structures consist of doubly charged hexanuclear 15-MC-5 complex cations and two nitrate anions providing the charge balance.

The model obtained from the single-crystal X-ray analysis of triclinic crystals of 3, space group $P\overline{1}$, is shown in Figure 5. There is a planar 15-membered ring with the repeating [Ni–O–N–] pattern and a Ca(II) ion inside the cavity. The coordination motif observed in 3 is typical for MC structures with α -hydroxamate ligands, but it is the first 15-MC-5 crystal structure obtained for **QuinHA**. The metallamacrocyclic cavity of 15-MC-5 is virtually planar, the Ca(II) ion deviates from the oxygens mean plane only by 0.026(1) Å. The cavity radius is

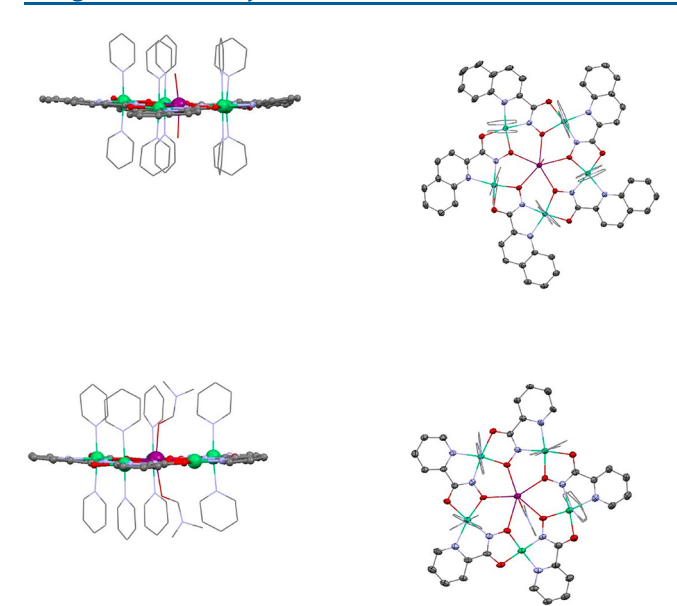


Figure 5. Crystal structure images of the $[CaNi_5(QuinHA-2H)_5(H_2O)_2(Pyridine)_{10}](NO_3)_2$, 3 (top), and $[CaNi_5(PicHA-2H)_5(DMF)_2(Pyridine)_8](NO_3)_2$, 4 (bottom). Color scheme: green = Ni, red = O, dark blue = N, gray = C, purple = Cl. Lattice solvent molecules and hydrogen atoms were removed; axial ligands are displayed as thin lines in the ball and stick diagram for clarity.

1.138 Å, which fits to the calculated ionic radius of Ca(II) (1.137 Å). The QuinHA ligand forms fused five-membered chelate rings, coordinating in a bis(chelating) mode via the carbonyl and hydroxamate oxygens to one Ni(II) ion, and through the hydroxamate and pyridine nitrogens to the second one. Each of Ni(II) ions of 3 is six coordinated; at the equatorial plane it is bonded by oxygen and nitrogen atoms from QuinHA, and in axial positions by N_{pyridine}, which completes the octahedral coordination geometry of metal ions. The core Ca(II) ion has a coordination number of 7, where five positions in the equatorial plane are occupied by the hydroximate oxygens and the last two by oxygens from water molecules. The Ni(II) ions form with QuinHA²⁻ a neutral MC ring, while positive charge from Ca(II) encapsulated in the center of the MC is balanced by two nitrate ions, which are present in the crystal lattice along with an unbound pyridine molecule (not shown).

The $[CaNi_5(PicHA-2H)_5(DMF)_2(Py)_8](NO_3)_2$, 4 was obtained as yellow-green monoclinic crystals, space group Cc. The crystallographic structure of 4 is similar to that of the related Cu(II) and Ni(II) complexes. $^{39,41,43,59-61}$

The 15-MC-5 of Ni(II) and **PicHA** with Ca(II) ion inside the cavity is only a little buckled. The core metal only slightly deviates from the oxygens mean plane (by 0.006(2)Å). The cavity radius is 1.137 Å which fits ideally to the calculated ionic radius of Ca(II) (1.138 Å). In both 3 and 4, these parameters are somewhat greater than those seen in [15-MC_(Cu,PicHA)-5] containing Ca(II) (1.067 Å for cavity radius and 1.066 Å for calculated ionic radius)³¹ that can be due to shorter Cu–O and Cu–N distances in the circuit as compare to Ni–O and Ni–N. As a consequence, the average Ca–O_{hydroximate} bond lengths in 3 and 4 (2.497 and 2.492 Å, respectively) are noticeably longer than those in Ca(II) [15-MC_(Cu,PicHA)-5] (2.426 Å).³¹ Four of five ring Ni(II) ions are octahedral, each additionally coordinated by two axial pyridine molecules

(Figure 5). The fifth Ni(II) ion is not bound to pyridine ligands and possesses square-planar geometry.

The distances for square-planar Ni(II) are distinctly shorter than the respective bonds formed by four octahedral Ni(II) ions (Table S5). The same "Ni pattern" (four octahedral and one square-planar Ni(II) ions in the 15-MC-5) was observed for the {Ln(III)[15-MC_{Ni(II),PicHA}-5]} obtained by Lisowski et al. ⁴³ Interestingly, in the case of Cu(II) as a ring metal, PicHA also forms nearly planar 15-MC-5 with Ca(II) as core metal, and the cavity sizes are very close, although the ionic radius of octahedral Ni(II) is larger than 5-coordinated Cu(II). Evidently, the incorporation of one square-planar Ni(II) ion with significantly shortened Ni–N and Ni–O bond distances into MC framework is necessary to decrease the cavity size to fit the ionic radius of Ca(II).

In general, by its nearly planar conformations and the values of Ca(II) deviation from OMP, the Ni(II)-Ca(II) 15-MC-5 are very close to the reported Cu(II)-Ca(II) analogs based on $PicHA^{39}$ and L-TrpHA. The most significant differences are connected with larger cavity size and the calculated Ca(II) ionic radius in Ni(II) MCs conditioned by larger ionic radius of the octahedral Ni(II) ions as compare to Cu(II) in the ring.

Molecular Structure of [Ni(PicHA-H)₂(Py)₂]·Py (5). With the use of metal-to-ligand 1:2 molar ratio, a mononuclear complex, which corresponds to [NiL2] species, found in solution and predominating in the pH range 4.5-7 (vide infra), has been obtained. The complex is crystallized in a monoclinic crystal system, space group C2/c. The central ion is situated on an inversion center, in an octahedral environment of six nitrogen donor atoms (Figure S1). The equatorial plane is formed by the pyridine and hydroximato nitrogen atoms belonging to two deprotonated hydroxamate ligands coordinated in a (N,N')-chelating mode. Of importance, the hydroxamate is N-coordinated and deprotonated, while the hydroxamic OH function remains protonated, i.e., an inversion of the order of deprotonation takes place, which is in line with the presented solution studies (vide infra). This is an important point as it shows that Ni(II), when provided with a choice of the hydroxamate chelate or a pyridyl imino chelate chooses the nitrogen based first coordination sphere over the oxygen rich environment.

Solution Speciation. The first part of this paper provided structural evidence for different species that may be present during the formation or decomposition of 12-MC-4 species made from α -functionalized hydroxamic acids **QuinHA** and **PicHA** with Cu(II) or Ni(II). In the following sections we will now relate these new species, with those previously reported, in order to understand the solution thermodynamic stability and mechanism of formation of this structure type.

Determination of Ligand Protonation Behavior. The acid dissociation constants (Table 2) for QuinHA, PicHA, and PyzHA ligands (Scheme 1) were determined by potentio-

Table 2. Acid Dissociation Constants, pK_a , of QuinHA, PicHA, and PyzHA Ligands

	QuinHA	PicHA		PyzHA	
	MeOH/ H ₂ O ^a	MeOH/ H ₂ O ^a	H_2O^b	MeOH/ H ₂ O ^a	H_2O^a
pK_{a1} pK_{a2}	2.10(1) 9.64(1)	2.20(2) 9.66(2)	1.64(1) 8.28(1)	2.04(1) 9.14(1)	1.93(1) 7.80(1)

^a25 °C, I = 0.1 M NaCl. ^b25 °C, I = 0.1 M KCl, ref 37.

Table 3. Complex Formation Constants (log β) of the Cu(II), Ni(II), and Zn(II) Complexes with QuinHA, PicHA, and PyzHA

	QuinHA	PicHA	PicHA	PyzHA	PyzHA
	MeOH/H ₂ O ^a	MeOH/H ₂ O ^a	H_2O^b	MeOH/H ₂ O ^a	H_2O^c
		Cu(II)			
[CuL] ⁺		10.23(2)	8.69 ^b	9.5(1)	
$[CuL_2]$		18.64(8)	17.67 ^b		
$[CuL(LH_{-1})]^-$		8.90(10)	9.17 ^b		
$[Cu_5(LH_{-1})_4]^{2+}$	43.56(7)	44.31(5)	38.65 ^b	39.4(2)	
		Ni(II)			
[NiL] ⁺	6.74(4)	8.24(1)	7.15 ^b	7.02(2)	6.64(2)
$[NiL_2]$		16.50(1)	13.78 ^b	14.01(1)	11.70(11)
[NiL ₃] ⁻	18.21(4)	22.89(3)	19.36 ^b	19.61(4)	17.80(4)
$[NiL(LH_{-1})]^-$	5.04(5)	7.84(1)	4.28 ^b	5.46(4)	5.43(1)
$[Ni_5(LH_{-1})_4]^{2+}$	19.35(3)				
$[\mathrm{Ni}_5(\mathrm{LH}_{-1})_5]$	20.43(7)	26.13(14)	14.92 ^b	19.03(10)	11.73(9)
		Zn(II)			
$[ZnL]^+$	5.95(4)	5.71(10)	5.29 ^b		
$[ZnL_2]$	12.53(4)	12.66(4)	10.41 ^b	10.15(4)	7.75(2)
$[ZnL_3]^-$		16.58(8)	13.75 ^b	14.68(6)	10.71(6)
$[ZnL(LH_{-1})]^-$		3.21(10)	1.93 ^b	2.39(4)	-0.57(2)
$[Zn(LH_{-1})_2]^{2-}$				-9.16(7)	
$[Zn_5(LH_{-1})_4]^{2+}$	13.94(6)	14.22(13)	9.63 ^b		1.37(14)
$[\operatorname{Zn}_5(\operatorname{LH}_{-1})_5]$				6.78(3)	

 a 25 °C, I = 0.1 M NaCl, solvent: MeOH/H₂O 80:20 w/w. b 25 °C, I = 0.1 M KCl, solvent: H₂O; see ref 37. c 25 °C, I = 0.1 M NaCl, solvent: H₂O.

metric titrations. Due to solubility reasons, complete physicochemical and thermodynamic characterization of ligands and their metal complexes was performed in MeOH/ $\rm H_2O$ (80/20 w/w) solution; for comparative purposes PyzHA was studied also in $\rm H_2O$.

All ligands exhibit two dissociation constants in the measured pH range regardless of solvent conditions. The first step, reflected by pK_{al} , is related to proton dissociation from the quinoline, pyridine, and pyrazine nitrogen atoms, respectively. In agreement with previous studies carried out for picHA, 36,37 the p K_{a1} values of QuinHA and PicHA are lower than those reported for quinaldine $(pK_a = 5.43, Table S8)^{63}$ or picoline (p $K_a = 6.12$, Table S8),⁶⁴ and very close to the p K_a reported for their corresponding carboxylic acids (p $K_a \approx 2$, 65,66 Table S8). The decrease of the pK_{a1} of the ligands may be explained by the presence of an $OH_{hydoxamic}$... N_{quinoline/pyridine/pyrazine} intramolecular hydrogen bond. For PyzHA, the pK_{a1} is higher than for both methylpyrazine $(pK_a = 1.45, Table S8)^{67}$ and 2-pyrazinecarboxylic acid $(pK_a from -0.7 to 0.9, Table S8)^{68-70}$ Although for the last compound there are large discrepancies between protonation constants presented in the literature (Table S8), it is clear that the presence of a second nitrogen in the aromatic ring reduces considerably the basicity of the ligand. However, this behavior is not so strongly reflected in PyzHA; in MeOH/ H_2O the p K_{a1} of PyzHA is only 0.1-0.2 log units lower than those of QuinHA and PicHA, while in H₂O it is 0.3 log units higher. The protonation of the pyrazine nitrogen may be influenced more by an inductive effect of the hydroxamate group, as well as hydrogen bond formation, than an electron withdrawing effect coming from the second nitrogen of the aromatic ring. The solvation effects due to the use of MeOH/H₂O mixture (80/20 w/w) may also play a role.

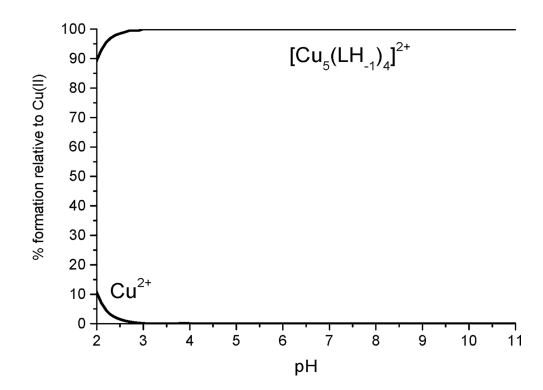
In the studied series, the pK_{a2} corresponds to the ionization of the proton of the hydroxamate group, and the constants

determined for all three ligands are comparable with the values previously observed for **PicHA** (measured under the same solvent conditions). An increase of the hydroxamate dissociation constants (by more than 1 log unit) in MeOH/ H_2O mixture is rather typical, and was previously observed also for α -aminohydroxamic acid ligands. Furthermore, the comparison of the dissociation constants, pK_{a2} , of the studied series shows that **PyzHA** is ca. 3 times (0.5 log units) less basic than **QuinHA** and **PicHA** (Table 2). All these data clearly indicate particular electronic accepting effects of the aromatic rings, which lead to reduction of the electron density of the hydroxamate groups and facilitate the dissociation of O–H protons.

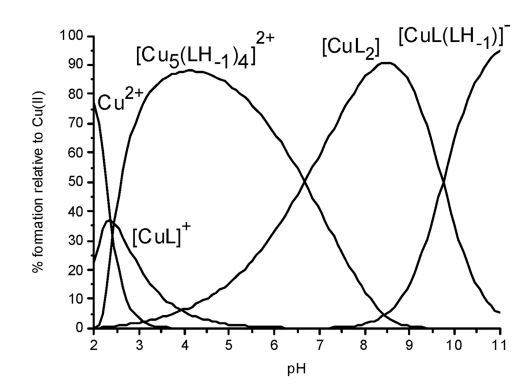
Cu(II) Complex Formation Equilibria. A satisfying fit of the potentiometric curves for the Cu(II)/QuinHA system was obtained using a model containing only one polynuclear complex, $[Cu_5(LH_{-1})_4]^{2+}$, throughout the entire measured pH range (Table 3, Figure 6). The speciation model obtained for the Cu(II)/QuinHA system is distinctly different from the model calculated previously for Cu(II)/PicHA, 36,37 which included $[CuL_2]^+$, $[CuL_2]$, and $[CuL_2H_{-1}]^-$ complexes. When these smaller species were introduced for the calculations with QuinHA, all speciation models were rejected by the program. Therefore, according to the calculations, the $[Cu_5(LH_{-1})_4]$ complex formation starts below pH 2 and dominates the speciation through pH 11.

In order to confirm the proposed model, we carried out ESI-MS experiments, with the spectra recorded for 1:1 and 1:3 metal-to-ligand ratios at pH 3.0 and 8.0. Indeed, only the Cu(II)(12-MC-4) complex and its adducts with chloride and perchlorate ions were detected: $[Cu_5(LH_{-1})_4]^{2+}$, m/z=530.40; $\{[Cu_5(LH_{-1})_4](Cl^-)\}^+$, m/z=1161.76 (Figure S3, Table S9). This finding is consistent with the ESI-MS spectra of the dissolved crystals of $\{Cu(II)[12-MC_{Cu(II),QuinHA}-4]\}^{2+}$ 1, which

a) Cu(II)/QuinHA



b) Cu(II)/PicHA



c) Cu(II)/PyzHA

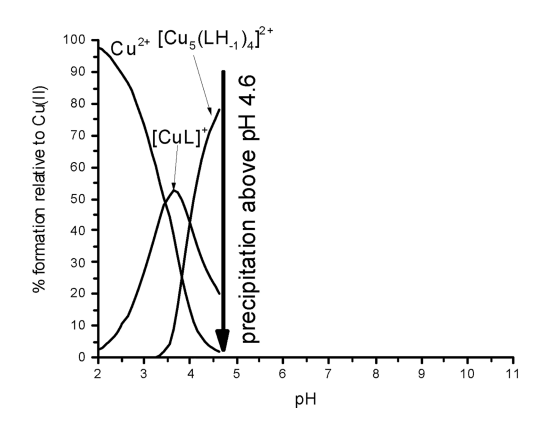


Figure 6. Representative distribution diagrams for the systems Cu(II)/QuinHA (a), Cu(II)/PicHA (b), and Cu(II)/PyzHA (c). Metal-to-ligand ratio of 1:2, $[L] = 3 \times 10^{-3}$ M, I = 0.1 M NaCl.

exhibited a peak at m/z 1122.81, corresponding to $\{(Cu_5(\mathbf{QuinHA})_4)^{2+}+NO_3^{-}\}^+$.

EPR and UV-vis spectroscopic experiments were also recorded in order to confirm the speciation model proposed for Cu(II)/QuinHA. The EPR spectra recorded at 77 K in the pH range 1.0–10.5 are silent from pH 2 to 10.5 (Figure S4), which strongly supports the model without mononuclear Cu(II) complexes that are expected to be EPR active. In the case of PicHA complexes, where in addition to 12-MC-4 species, the formation of mononuclear complexes was

observed, the EPR characteristics were different, with a signal at A_{\parallel} = 196 G and g_{\parallel} = 2.22 reappearing above pH 5, that corresponded to the $\{4N\}$ binding mode of the CuL_2 -type complexes. The lack of EPR signal is typical for polynuclear Cu(II) species, and was found also for the majority of Cu(II) 12-MC-4 complexes. 73,74 To date only two of all the polynuclear Cu(II) 12-MC-4 species studied by EPR were not EPR-silent, but in these cases the spectra were both measured at 4-6 K. 75,76 To verify the solution EPR behavior, we measured EPR spectra (at 77 K) for the dissolved crystals of $\{\text{Cu}(\text{II})[12\text{-MC}_{\text{Cu}(\text{II}),\text{QuinHA}}\text{-}4]\}^{2+}$ 1 and, once again, we did not observe any detectable signal in the EPR spectra (Figure S5). This indicates that under these solution and temperature conditions this pentanuclear Cu(II) complex is not EPR active. In some ways this is surprising as previous magnetic studies of Cu(II) metallacrowns have indicated that the ring metals are antiferromagnetically coupled, leading to an S = 0 ground state for the 12-MC-4 ring.⁷⁷ In this scenario, the remaining central Cu(II) ion is expected to be S = 1/2, giving the complex a total S = 1/2 spin. The lack of an EPR signal suggests that relaxation phenomena, and not the ground spin state, is the reason for this EPR silent behavior. The addition of HCl to the EPR sample resulted in an EPR spectrum characteristic of the uncomplexed Cu(II) in solution (Figure S5). These observations are consistent with the proposed speciation model lacking mononuclear complexes.

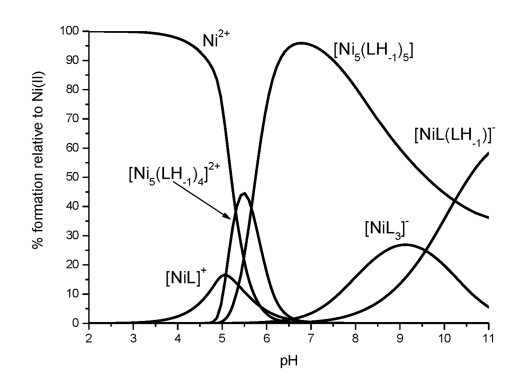
Although UV–vis spectra, could not provide sufficient information to characterize the complex species fully, they confirm the formation of a Cu(II)-hydroxamate complex through the presence of (i) high energy, intense, ligand-to-metal charge-transfer transitions, LMCT, previously attributed to N $^-$ -O $^-$ (nitrogen) \rightarrow Cu(II) and N $^-$ -O $^-$ (oxygen) \rightarrow Cu(II) CT transitions, $^{12,7/8}$ ($\varepsilon_{395}=1.64\times10^4$ M $^{-1}$ cm $^{-1}$, calculated assuming the $\left[\mathrm{Cu}_5(\mathrm{LH}_{-1})_4\right]^{2^+}$ as the only species), and (ii) d-d bands at 550 nm (observed above pH 3), even if the d-d bands are only observed as shoulders (Figure S6).

Due to solubility problems (a precipitation occurs above pH 4.6), the speciation model and formation constants of Cu(II)/ PyzHA complexes could not be determined directly from the potentiometric titrations; therefore, an indirect method (i.e., the pH-dependent UV-vis titration in the d-d range) was used. First, the presence of $[CuL]^+$ and $[Cu_5(LH_{-1})_4]^{2+}$ complexes was identified by ESI-MS spectra, dominated by the signals of the $[CuL]^+$ (m/z = 200.96), $\{(Ca^{2+})^ Cu_5[(LH_{-1})_5]^{2+}$ (m/z = 520.86) and $[Cu_5(LH_{-1})_4]^{2+}$ $(m/z)^{2+}$ = 432.37) (Figure S7, Table S9). Based on this data, the model with two species, $[CuL]^+$ and $[Cu_5(LH_{-1})_4]^{2+}$, was assumed. The stability constant of the first formed species, $[CuL]^+$, $\log \beta$ = 9.5(1), was estimated from the spectrophotometric pHdependent titration, carried out in a pH range of 2.3-3.0 (Figure S8a). This value, together with data from the electronic spectrum of the [CuL]⁺ complex ($\varepsilon_{719} = 98 \text{ M}^{-1}$ cm⁻¹, Figure S8c), were further used as fixed in the calculations of the formation constant of $[Cu_5(LH_{-1})_4]^{2+}$ species, $\log \beta =$ 39.4(2), from the spectrophotometric titration carried out in a pH range from 2.5 to 4.6 ($\varepsilon_{575} = 645 \text{ M}^{-1} \text{ cm}^{-1}$, Figure S8b,c). Above pH 4.6 a precipitation occurred, even at the concentration of PyzHA = 2×10^{-4} M. Overall, the speciation model could be proposed only up to pH 4.6, with the formation of two complexes: [CuL]⁺ and [Cu₅(LH₋₁)₄]²⁺ (Table 3, Figure 6). Unfortunately, due to the low concentration of the reagents used, the EPR spectra are not of good quality (Figure S9), but as the EPR spectra are silent,

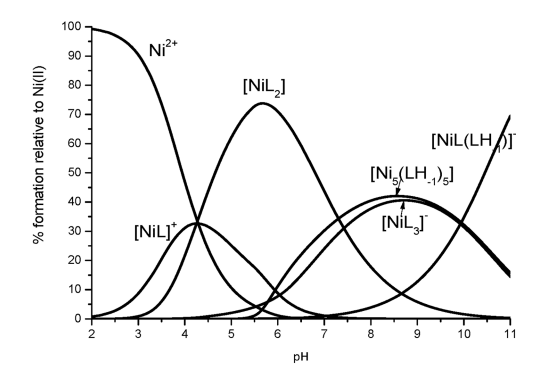
they clearly indicate that the mononuclear species is not observed in solution over the pH range 3.9-4.6.

Ni(II) Complex Formation Equilibria. For the Ni(II)/QuinHA system, the calculated speciation model contains a number of mono- and polynuclear species (Table 3, Figure 7a). The complexation starts with the mononuclear [NiL]⁺,

a) Ni(II)/QuinHA



b) Ni(II)/PicHA



c) Ni(II)/PyzHA

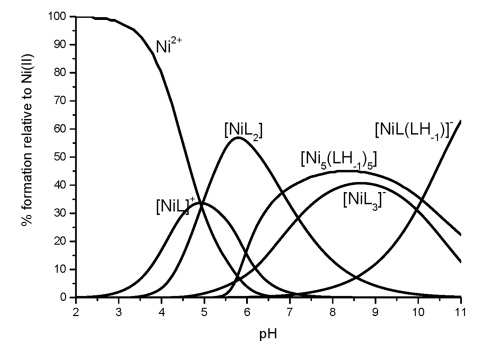


Figure 7. Representative distribution diagrams for the systems Ni(II)/QuinHA (a), Ni(II)/PicHA (b), Ni(II)/PyzHA (c). Metalto-ligand ratio of 1:2, $[L] = 3 \times 10^{-3}$ M, I = 0.1 M NaCl (MeOH/ $_{10}$ O 80/20 w/w).

followed by the formation of the polynuclear $[Ni_5(LH_{-1})_4]^{2-}$ (12-MC-4) complex present in a rather narrow pH-range (5–6.5), the behavior typical for Ni(II) 12-MC-4 complexes. ^{34,35} The formation of 12-MC-4 is almost concomitant with another polynuclear $[Ni_5(LH_{-1})_5]$ (15-MC-5) complex, predominating in the pH range 6–10. Starting from pH 7, $[NiL_3]^-$ and $[NiL(LH_{-1})]^-$ species occur together with the 15-MC-5

complex until pH 11. The formation of both polynuclear complexes was confirmed by ESI-MS spectra, which reveal the presence of two major peaks successfully attributed to $\{[Ni_5(LH_{-1})_4](Cl^-)\}^+$, m/z=1072.81, and $\{(Na^+)-Ni_5[(LH_{-1})_5]\}^+$, m/z=1246.87 species (Figure S10, Table S9). UV—vis characteristics of the system are given in Figure S11. The presence of both 12-MC-4 and 15-MC-5 species, is expected given that the crystal structure of the 12-MC-4 complex was reported, 40 and crystals of 15-MC-5 obtained from a DMF-pyridine solution are discussed herein (vide supra).

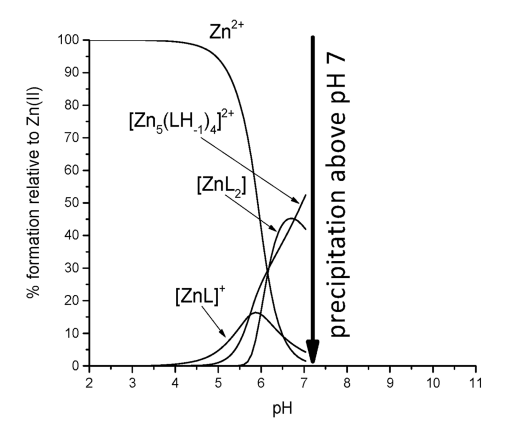
Ni(II)/PicHA system was previously studied in H₂O solution,³⁷ and the results indicated the formation of a 15-MC-5 complex as a unique MC species. For a better comparison, we reinvestigated the Ni(II)/PicHA system under our experimental conditions, i.e. in MeOH/H2O mixture (80/20 w/w). The speciation model is presented in Table 3, and the corresponding distribution diagram is given in Figure 7b. The ESI-MS (dominated by $\{(Na^+)[Ni_5(LH_{-1})_5]\}^+$, m/z = 994.80, Figure S12, Table S9), and spectral characteristics of the system are given in the SI. Importantly, as in H₂O solution, the formation of the 12-MC-4 complex is not observed in MeOH/H2O mixture. It should be emphasized that the presence of MeOH in the solution significantly increases $\log \beta$ of Ni(II)-PicHA 15-MC-5 compared to H₂O solution (26.13 versus 14.92, respectively); this issue was already discussed on PicHA and other examples.²⁹ It is worth mentioning that for both of the solvent systems described above, the formation of a Ni(II) 15-MC-5 complex strongly depends on the metal-to-ligand ratio, and it is observed only at Ni(II)-to-**PicHA** ratios $\leq 1:2$. The best fitting of the measurements performed with a Ni(II)-to-PicHA molar ratio of 1:3 was obtained with a speciation model containing only mononuclear complexes [NiL]+, [NiL2], [NiL3]-, and [NiL- (LH_{-1})] (Table S10, Figure S13). This behavior is in agreement with the results reported previously for α -AlaHA, ValHA, β-AlaHA. 34,35 Here again, the presence of 15-MC-5 and NiL2 species is in agreement with the structures of the crystallized solid compounds (vide supra).

The speciation model of the Ni(II)/PyzHA system is very similar to Ni(II)/PicHA, both in MeOH/H₂O and H₂O, and contains mononuclear and polynuclear species (Table 3, Figure 7c, Figure S15). In both solvents, an introduction to the speciation model of 12-MC-4, either an exclusion of the 15-MC-5 led to a lack of fitting of the potentiometric curves. The formation of the 15-MC-5 was confirmed by ESI-MS ($\{(Na^+)Ni_5[(LH_{-1})_5]\}^+$, m/z = 999.78, Figure S16, Table S9); no signals attributed to the 12-MC-4 species were observed.

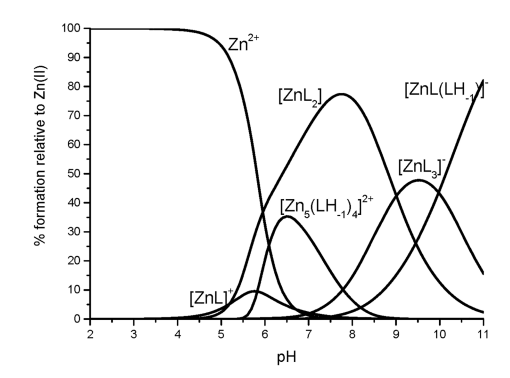
Zn(II) Complex Formation Equilibria. For the Zn(II)/QuinHA system the collection of the potentiometric data was limited to pH 7, due to a precipitation occurring above this pH. The speciation model consists of mononuclear, $[ZnL]^+$ and $[ZnL_2]$, and the 12-MC-4 ($[Zn_5(LH_{-1})_4]^{2+}$) species (Table 3, Figure 8). The ESI-MS experiments confirm the presence of 12-MC-4 complex in solution ($[Zn_5(LH_{-1})_4]^{2+}$, m/z = 535.90, Figure S19, Table S8).

The interactions between Zn(II) and **PicHA** ligand were previously examined in aqueous solution, ³⁷ and the speciation model obtained for comparison under current experimental conditions (MeOH/ H_2 O mixture, 80/20 w/w) is very similar (Table 3, Figure 8). Again, ESI-MS spectra confirm the existence of 12-MC-4 complex ({[Zn₅(LH₋₁)₄](Cl⁻)}+ (m/z = 906.71) (Figure S20, Table S8). Of importance, the crystal

a) Zn(II)/QuinHA



b) Zn(II)/PicHA



c) Zn(II)/PyzHA

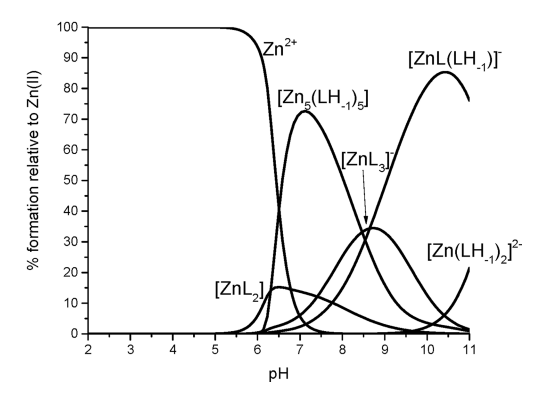


Figure 8. Representative distribution diagrams for the systems Zn(II)/QuinHA (a), Zn(II)/PicHA (b), Zn(II)/PyzHA (c). Metal-to-ligand ratio of 1:2, $[L] = 3 \times 10^{-3}$ M, I = 0.1 M NaCl (MeOH/H₂O 80/20).

structures of both Zn(II)/QuinHA and Zn(II)/PicHA 12-MC-4 were obtained from the DMF-pyridine solution, with pyridine molecules coordinated to the axial positions of Zn(II).

Depending on the solvent conditions, two different MCs needed to be introduced in the speciation models for the Zn(II)/PyzHA system, namely the 15-MC-5 $[Zn_5(LH_{-1})_5]$ in MeOH/H₂O mixture, and 12-MC-4 $[Zn_5(LH_{-1})_4]^{2+}$ in H₂O. In addition to these complexes, introduction of a number of mononuclear species was required to obtain a satisfactory fitting of the potentiometric curves (Table 3, Figure 8, Figure

S21). In MeOH/H₂O solvent, we were not able to obtain good fitting without the 15-MC-5 species. Attempts to introduce the 12-MC-4 alone led to a total lack of fitting of the curves. If treated by the 12-MC-4 together with 15-MC-5, the convergence process resulted in the rejection of the 12-MC-4 species. Therefore, based on the potentiometric data treatment, we propose for Zn(II)/PyzHA system the two speciation models reported in Table 3. The presence of the 15-MC-5 complex was very surprising for us, especially since we are not able to confirm this species by ESI-MS spectra. However, the signals on the ESI-MS spectra of Zn(II)/PyzHA are of low intensity (Figure S22), and even if collected several times (on several different samples), only the signals attributed to the $[ZnL]^+$ (m/z = 201.95) and $[Zn(LH)L]^+$ (m/z = 341.00) (Table S9) could be identified.

DISCUSSION

Ni(II), Cu(II), and Zn(II) all form polynuclear complexes with the described ligands, QuinHA, PicHA, and PyzHA, with various topologies and thermodynamic stabilities, depending on the type of metal ion and ligand. From the three compounds, the QuinHA ligand has a unique behavior with Cu(II) and Ni(II), as it forms a Cu(II) 12-MC-4 complex along the entire pH range, and Ni(II) 12-MC-4, the latter not observed for PicHA nor PyzHA ligands.

The low basicity, and availability of the deprotonated quinoline nitrogen of QuinHA for Cu(II) ions at acidic pH, allows for the formation of Cu(II) complexes starting at pH 2 (Figure 6). A very similar behavior was observed for Cu(II)/ **PicHA** and Cu(II)/**PyzHA** systems, while for a series of α aminohydroxamic acids the complexation usually starts 2 pH units higher.³⁷ The stability of the 12-MC-4 $\left[Cu_5(LH_{-1})_4\right]^{2+}$ complexes of QuinHA and PicHA are comparable, $\log \beta$ of 12-MC-4 of QuinHA is only 0.75 log units lower than that of **PicHA** under the same experimental conditions (Table 3). The comparison of log β of the 12-MC-4 $\left[Cu_5(LH_{-1})_4\right]^{2+}$ complex of PyzHA reveals that it is evidently less stable than those of QuinHA and PicHA (4.16–4.91 log units). The lower stability of the PyzHA complex is probably a consequence of the stronger π -acceptor properties of the ligand and lower basicity of its hydroxamate group. ⁷⁹ The Cu(II)/PicHA system was reexamined in MeOH/H₂O solution, providing slightly different thermodynamic data than reported earlier. ³⁶ Indeed, the log β of Cu(II)/PicHA 12-MC-4 is not the highest determined until now, but still we should underline the significant impact of the use of organic solvent on the stabilization of the MC complexes. ⁷² Overall, the stability of Cu(II)/QuinHA, Cu-(II)/PicHA, and Cu(II)/PyzHA 12-MC-4 complexes is lower than analogous compounds of α -aminohydroxamic acids, i.e., (S)-phenylalaninehydroxamic acid, PheHA, and (S)-tryptophanhydroxamic acid, TrpHA, obtained in MeOH/H2O 9:1 v/v solvent, with log β of 51.58 and 52.37, respectively.⁷² The same trend is observed when we compare $\log \beta$ values of the $[Cu_5(LH_{-1})_4]$ of **PicHA** and **AlaHA** ligands in H_2O solution; they are 38.65 and 40.16, respectively.³⁷ As discussed by Tegoni et al., the Cu(II) 12-MC-4 with PicHA is less stable than that with AlaHA due to (i) the different nature of the donor groups (pyridyl versus amino), and (ii) more highly strained framework of the PicHA 12-MC-4 with relation to AlaHA analog.37

We assume that the very close stability of QuinHA and PicHA Cu(II) 12-MC-4 complexes comes from electronic similarity of the ligands. Although, until now numerous

$$[Cu_4(\textbf{PicHA-}2H)_2(\textbf{PicHA-}2H)_2]^{2^+}$$
 collapsed MC fragment of $[Cu_{10}(\textbf{PicHA-}2H)_8(H_2O)_4(ClO_4)_3]^+$ $[Cu_5(\textbf{PicHA-}2H)_4]^{2^+}$

Figure 9. Possible options of metal ion uptake by collapsed MCs.

attempts to isolate Cu(II) 12-MC-4 with PicHA in the solid state were unsuccessful, the corresponding complex with QuinHA (1) has been obtained. Therefore, to compare the structure of the two complexes, we have overlaid the structure of 1 with the optimized molecular structure of Cu(II) 12-MC-4 with PicHA³⁷ (Figure S2). Both structures exhibit a similar bowl shape, with the central Cu(II) located at the bottom. The main difference is in the depth and width of the concave cavity, which is greater for 1 due to larger size of the QuinHA ligand. Taking into account the information from speciation studies, and the presence of pentanuclear units with alternative, non-12-MC-4 topology, in the structure of 2, it is possible to consider an existence of both types of isomeric species (12-MC-4 and non-12-MC-4, Figure 9) in solution. Actually, these species cannot be distinguished in solution, as their spectral characteristics are expected to be very similar (UV-vis) or identical (EPR, ESI-MS). They should exhibit different stability constants, but it is believed that their values should be strongly solvent-dependent. If the isomeric species are present in comparable amounts, the observed stability constant is in fact a combined value of contributions from two different species. Significant difference in the values of stability constants of 5:4 species with PicHA in pure water and mixed aqueous—methanol solution (vide infra) can be due to a predominant presence of one isomeric form. Evidently, as demonstrated before and in the present work, the nature of the solvent plays a critical role in speciation, as in non-aqueous or mixed solutions the formation of collapsed species is favored.

We cannot either confirm or rule out the presence of this non-12-MC-4 species in aqueous solution, as numerous attempts to crystallize Cu(II) PicHA-containing 12-MC-4 from aqueous solutions have been unsuccessful, while the products obtained as a result of recrystallization from nonaqueous solvents (DMSO, DMF, alcohols) resulted in isolation of complexes with collapsed MC motifs. The presence of stoichiometrically excessive Cu(II) ions can result in exocoordination to the collapsed MC complex with the help of (O, O') vacant chelating unit, with consequent aggregation of the formed pentanuclear species in the course of crystallization of 2. However, ESI-MS spectra of all these PicHA-containing complexes dissolved in methanol always indicated the presence of both tetranuclear (collapsed MC) and pentanuclear (12-MC-4 or collapsed MC with an exo-coordinated Cu(II) ion) species, with the signals from the latter being the most intensive (100% in all the cases). On the contrary, in ESI-MS of solutions containing Cu(II) salts and QuinHA, 4:4 species corresponding to collapsed MC, have never been observed, as well as in the case of a methanolic solution of 1. Only 5:4

species have been registered in ESI-MS spectra of these systems (vide supra).

Comparing the speciation model calculated for Ni(II)/QuinHA to those reported for Ni(II)/PicHA and Ni(II)/PyzHA systems, it is easy to note the presence of an additional MC complex, 12-MC-4, beside 15-MC-5. The coexistence in solution of both Ni(II) 12-MC-4 and 15-MC-5, complexes were previously observed for α -AlaHA, ValHA, and β -AlaHA.^{34,35} The formation of solely 15-MC-5 in the Ni(II)/PicHA system in aqueous medium was rationalized by stabilization of a square planar coordination of Ni(II) ions, reflected by higher log β (14.92 versus 13.53 for α -AlaHA, and 13.9 for ValHA).^{34,35} Moreover, the lack of the 12-MC-4 Ni(II)/PicHA complex was explained by the lower flexibility of the ligand in comparison to α -AlaHA or ValHA.^{34,35}

The comparison of the stability constants of Ni(II)/ QuinHA and Ni(II)/PicHA systems reveals a few orders of magnitude increase in the stability of 15-MC-5 Ni(II)/PicHA complex (20.43 versus 26.13, respectively, Table 3). The higher $\log \beta$ of the 15-MC-5 Ni(II)/PicHA does not allow for a significant amount of 12-MC-4 species to form. The difference between log β of Ni(II)/QuinHA 12-MC-4 and 15-MC-5 is 1.08 in favor of the 15-MC-5, very close to the values observed for Ni(II)/ α -AlaHA, Ni(II)/ValHA, and Ni(II)/ β -AlaHA (1.89, 1.67, and 1.02, respectively), even though the 12-MC-4 complexes were more stable in the case of aliphatic ligands. 34,35 Moreover, the strong preference of the QuinHA ligand for the formation of MC species in solution is underlined by the fact of MC formation regardless of the metal-to-ligand ratio (Figure S18). For the Ni(II)/ α -AlaHA, Ni(II)/ValHA, and $Ni(II)/\beta$ -AlaHA the formation of MC complexes were observed only when the required metal-toligand ratio, namely below 1:2, was provided. 34,35 Here again, we may relate the higher tendency of the Ni(II)/QuinHA to form MCs with the higher hydrophobicity of the structure (in comparison to the Ni(II)/PicHA analogue), which seems especially important for the formation of 12-MC-4. Indeed, the formation of 12-MC-4 Ni(II)/QuinHA was confirmed by its successful isolation in the solid state. 40 Although a high degree of similarity exists between QuinHA and PicHA ligands, the corresponding Ni(II)/PicHA has not yet been isolated. In the crystal structure of 12-MC-4 Ni(II)/QuinHA, the presence of two axial pyridines coordinated to each peripheral Ni(II) ion are supposed to stabilize the structure, 40 alleviating the structural strains expected from the ab initio calculations of the putative 12-MC-4 complex formed by Ni(II)/PicHA pair.³⁷ Of importance, under the speciation conditions (MeOH/ H_2O , 80/20 w/w), the 12-MC-4 complex of Ni(II)/QuinHA forms in the absence of pyridine. It might

Figure 10. Scheme of a possible assembly pathway of the formation of 12-MC-4 and 15-MC-5 complexes. The central M(II) ion is displayed in green, the core M_4L_2 ligands are displayed in red, and the exogenous ligands in the M_4L_4 are displayed in blue.

be, that the stabilization of the MC complex could be obtained with the help of water or Cl⁻ ions (which are present in solution in high excess, 0.1 M).

The structures of the 15-MC-5 of both Ni(II)/QuinHA and Ni(II)/PicHA indicate nearly planar conformations with the Ca(II) ion residing perfectly within the MC cavity, with minimal differences in geometrical parameters in both structures. As for the Cu(II)/PyzHA system, the lower stability of the Ni(II)/PyzHA complexes in relation to Ni(II)/PicHA could be explained by the differences in donor properties of the ligands.

The complex formation constants of the Zn(II) 12-MC-4 complexes with **QuinHA** and **PicHA** are very close, with the slightly lower stability for the Zn(II) complexes of the former ligand (Table 3). Therefore, the presence of the additional aromatic group in the **QuinHA** ligand structure does not seem

to affect significantly on the stability of the Zn(II) MC complex. When comparing the stability constants of 12-MC-4 Zn(II)/PyzHA with the corresponding ones of PicHA and α -AlaHA ligands reported previously (all in H₂O solvent),³⁷ much lower stability of Zn(II)/PyzHA is evident; its log β is ~8.3 orders of magnitude lower than that of PicHA (Table 3), and ~5.4 of α -AlaHA (log β = 6.79).³⁷ It is very difficult to explain the presence of the 15-MC-5 Zn(II)/PyzHA complex in MeOH/H₂O solution. This behavior could be due to a strong influence of the solvent on the ligand and its complexes. It should be mentioned that in absence of Ln(III) ions, Zn(II) 15-MC-5 complexes were not isolated in the solid state to date.⁴⁰

Overall, taking into account the three studied ligands, and three metals, the following general rationale could be observed. **QuinHA** has the highest propensity to the formation of the

Figure 11. Comparison of PicHA and QuinHA collapsed MCs.

 $[Cu_4(PicHA-2H)_2(PicHA-H)_2]^{2+}$

MC structures, both in solution and in the solid state. It forms the most stable MC complex with Cu(II), for which the Cu(II) 12-MC-4 predominates in solution over the entire pH range. The isolation of Cu(II) 12-MC-4, 1, in solid state confirms the predisposition of QuinHA to the formation of Cu(II) 12-MC-4. Although other species, i.e., Ca(II) 15-MC-5, could be detected by ESI-MS, their formation in solution was not detected by potentiometry. As regards the stability of Cu(II) 12-MC-4 in relation to the other two metals, it is the highest for Cu(II) (log β = 45.56), followed by Ni(II) (log β = 19.35) and Zn(II) (log β = 13.94). This is rather classical behavior for the three metal ions, due to lower affinity of Ni(II) and Zn(II) ions toward O and N donor atoms with respect to Cu(II); the same behavior was earlier observed for α -AlaHA and ValHA 12-MC-4. 34,35 It has to be emphasized that it is very difficult to compare the speciation of the three metals, as the thermodynamic stability of 12-MC-4, is not the only parameter reflecting the ability of the ligand to form MC complexes. The comparison of the species distribution diagrams presented in Figures 6-8, clearly shows that in these systems the speciation models are usually complicated, with MC complexes present in a rather narrow pH range, being in equilibria with other monoand multinuclear species. Of importance, Cu(II)/QuinHA is the only example among α -hydroximate compounds, that 12-MC-4 is the only species formed in solution. For Ni(II), 12-MC-4 forms in solution just before another MC, 15-MC-5 (Figure 7). Here again the QuinHA ligand is very exceptional, as for its close analogue PicHA, Ni(II)(12-MC-4) were not formed in solution nor isolated in the solid state. The very close log β values for 12-MC-4 and 15-MC-5 of Ni(II)/ QuinHA (Table 3) and predomination of Ni(II) 15-MC-5 in solution of both ligands might suggest that Ni(II) 12-MC-4 may be only a transient species in the formation of the larger, more sterically convenient Ni(II) 15-MC-5. Finally, Zn(II) forms mainly 12-MC-4 complexes, and the presence of 15-MC-5 for PyzHA in MeOH/H₂O solvent needs to be checked under conditions of other background salts and, if possible,

Overall, the solution studies carried out here in MeOH/ H_2O solvent, used for solubility reasons, allowed us to describe the formation of complexes of **QuinHA** ligand, and compare the data to **PicHA** studied earlier in water, revealing analogous equilibria. At the same time, they reveal that steric factors depending on the size of the ligands, ability of π -electron clouds to interact, as well as a very subtle solvation effects due to the differences in hydrophobicity of the ligands, pH, and

confirmed by isolation of corresponding crystals.

anions could influence the stability of corresponding structures. In the light of the described equilibria and solid state data, we may claim we have found a perfect match: Cu(II)/QuinHA system, for which the changes in size and hydrophobicity of the ligand led to a very stable, predominating over pH 2–11, Cu(II)(12-MC-4) complex.

 $[Cu_4(QuinHA-2H)_2(QuinHA-H)_2]^{2+}$

It is well known that when the proper conditions (metal-toligand molar ratio, pH etc.) are used, MCs form spontaneously in solution with no need to synthesize precursors of the final supramolecular entity. To date, one of the main goals of MC research has been to propose possible pathways of MC selfassembly and identification of the building blocks leading to the final, most stable MC species. In 2013, Pecoraro et al. proposed a possible assembly pathway of the formation of 12-MC-4 complex as the thermodynamically favored product (Figure 10a-e). It is very difficult to definitively affirm or refute this mechanism, but the structural data obtained to date for Cu(II), Ni(II), and Zn(II) complexes with PicHA, as well as solution speciation studies are in good agreement with the presented pathway. Indeed, results described in the current paper can complete the scheme and, in addition, we can propose the next step leading to the formation of 15-MC-5 (Figure 10f,g). It should be emphasized, that the collapsed MC fragment of $[Cu_{10}(PicHA-2H)_8(H_2O)_4(ClO_4)_3](ClO_4)$. 4H₂O, 2, presented herein is in a perfect agreement with the proposed intermediate 10d, which has not previously been identified by experimental data. By the characterization of this complex we supplement the missing link of the scheme of 12-MC-4 self-assembly, further supporting this mechanism. According to structure 2, we can propose a modification of the product 10d toward exo-(O,O')-chelate bonding mode instead of monodentate exo-coordination of the metal ion. Moreover, the comparison of the conformation of the collapsed 12-MC-4 proposed in ref 34 (10c) to the present structure, 2, reveals key differences. While the collapsed moiety is nearly planar, in 2 we note a significant twist between the two halves of the structure, vide supra. This twist provides the necessary space for exo-chelation. Actually, as discussed above, the two most important isomeric species (non-12-MC-4 and 12-MC-4, Figure 10d,e) might not be distinguished in solution; the pentanuclear exo-coordinated non-12-MC-4 complex might be an important participant of equilibria, and not just a transient short-lived species, whose presence depends on organic solvent content. Its isolation could be a result of reaching an appropriate crystallization condition,

which could not be realized during potentiometric investigations (pure organic solvent).

It seems that in the case of QuinHA, the exo-chelation of an extra metal ion with the help of vacant (O, O') chelating unit is not possible due to steric hindrances (spatial proximity of hydroxy and oximato oxygens, and benzene rings, Figure 11). Moreover, the formation of a collapsed MC in the case of QuinHA seems to be highly implausible or even impossible due to the above-mentioned steric peculiarities. Consequently, this can be a reason for additional stabilization of the pentanuclear 12-MC-4 structure with QuinHA, as the possible pathways of degradation and rearrangements are eliminated. This means that the formation of QuinHA-containing 12-MC-4 should not proceed according to the mechanism discussed above, 32 through envisaged formation of intermediate tetranuclear collapsed and pentanuclear non-MC exo-chelated species, but by an alternative pathway. It may involve the formation of N,N'-coordinated mononuclear 1:1 species followed by consequent templating of four of them around a Cu(II) aqua ion.

The structural characterization of $[CaNi_5(QuinHA-2H)_5(H_2O)_2(Pyridine)_{10}](NO_3)_2$, 3, and $[CaNi_5(PicHA-2H)_5(DMF)_2(Pyridine)_8](NO_3)_2$, 4, together with the speciation studies on the formation of Ni(II) MCs, inspired us to take a step forward, into the rearrangement of 12-MC-4 to 15-MC-5. This transition is in line with the speciation studies identifying the Ni(II) 15-MC-5 complex as the thermodynamically favored product. The small ionic radius of Ni(II), as well as geometrical preferences of this metal ion might result in the destabilization of the strained Ni(II) 12-MC-4 scaffold and make them a transition building block in the assembly of most convenient Ni(II) 15-MC-5. Here, a Na(I) or other background ions present is solution might play a templating role. 27

The assembly of MCs could reasonably proceed through multiple pathways and consist of more intermediates (not only poly- but also mononuclear), but we could be sure that the proposed final products -12-MC-4 (in case of Cu(II) and Zn(II)) or 15-MC-5 (for Ni(II)) are the most thermodynamically stable polynuclear species characterized by the speciation studies. Correlation between the species isolated in solid state and those thermodynamically stable in solution brings us closer to confirm possible mechanism of MCs formation.

CONCLUSIONS

Our results underline the peculiar influence of the ligand structure, the nature of metal ions, and axial ligands on the formation of the metallacrown complexes with different topologies and stability. To design new MCs with desired stabilities and predetermined topologies and conformation, numerous aspects should be taken into account, such as the basicity, size (in particular, bulkiness), geometry or aromatic character of the ligands, the geometrical preferences of the metal ions, nature, size and denticity of the potential axial ligands, as well as choice of solvent and solvation effects. All of the above parameters have an influence on the strong preference of the QuinHA ligand for the formation of MC species in solution, especially Cu(II) MC complex, which is the first example of the system with the presence of only one, 12-MC-4, complex dominating in solution over the whole pH range. Taking into account the information from speciation studies, it might be that the van der Waals interaction of π electron clouds and hydrophobicity of the structure play a crucial role, with methanol solvent stabilizing the

 $\left[\operatorname{Cu}_{5}(\operatorname{LH}_{-1})_{4}\right]^{2+}$ complex over entire pH range at the expense of mononuclear CuL and CuL2 complexes. Isolation of two different MC crystal structures with Cu(II) ions from organic solvents, i.e. (i) $[Cu_5(QuinHA-2H)_4(NO_3)(DMSO)_4](NO_3)$, obtained from DMSO, and corresponding to $\left[Cu_5(LH_{-1})_4\right]^{2+}$ complex form predominating in entire pH range of MeOH/ H_2O solution, and (ii) $\left[Cu_{10}(PicHA-2H)_8(H_2O)_4(ClO_4)_3\right]$ (ClO₄), consisting of two collapsed MC Cu₄(PicHA-2H)₄ fragments united by two Cu(II) ions, stoichiometrically corresponding to [Cu₅(PicHA-2H)₄]²⁺, but never isolated in this form, as well as the fact of earlier isolation of collapsed MC, [Cu₄(PicHA-H)₂(PicHA-2H)₂](ClO₄)₂·2DMF, after dissolution of Cu₅(PicHA-2H)₄(ClO₄)₂·6H₂O in organic solvents,³⁴ suggests existence of not only complicated solvent-dependent equilibria in solution (between the tetraand pentanuclear species), but probably also between the solution and solid phase of growing crystals.

The strong preference of **QuinHA** for the formation of MC species was also reflected in the formation of Ni(II)/ **QuinHA** MCs, when 12-MC-4 and 15-MC-5, predominating in solution in a wide pH range, were formed in solution regardless the metal-to-ligand ratios. On the other hand, our results are in line with the geometric preferences and the ionic radii of the coordinated metal ions. Ni(II), which is the smallest ion of the series examined and requires a square planar coordination, forms with **PicHA** and **PyzHA** only a 15-MC-5 species. Both, coordination preferences of Ni(II) ions and geometry of the **PicHA** and **PyzHA** disfavor the formation of 12-MC-4 species at the expense of rearrangement to most thermodynamically favored 15-MC-5. The present case once again demonstrates the difficulties in obtaining 12-MC-4 complexes using α -functionalized hydroxamates.

The diversity of coordination patterns observed in the isolated complexes and in thermodynamic studies confirms the potential of α -hydroxamic acids and makes them very promising ligands in coordination chemistry. Extension of the knowledge on the thermodynamics of the MCs formation, and a deeper understanding of the relationship between the structure of the ligands and the type of metal ions in an aspect of stability of the MC species have significance in the aspect of a potential use of MCs as functional materials or their precursors, in particular, biomedical materials (such as contrast agents, selective metal ion chelators or fluorescent probes), MC-based porous MOFs for selective sorption of various guest molecules, and SMM. Development of such MC or their assemblies with specific target properties for certain applications often requires further functionalization and complication of the ligand structures (such as introducing of fluorescent or electrochemically active modules, additional chelating and bridging units, pharmacophore compartments, etc.). Our spectacular examples clearly demonstrate how even subtle structural differences in peripheral, non-donor moieties of otherwise very similar α -hydroxamic acids can have a dramatic effect on complex formation behavior and structure of complexes crystallized in solid state. Evidently, further investigations with a wider set of α -hydroxamic acids are necessary to clarify the role of substituents. The proper molecular design of (multi)functional MC-based materials would require taking into account the full miscellany of factors determining the processes of self-assembly of these highly flexible, self-tunable systems.

ASSOCIATED CONTENT

S Supporting Information

The Supporting Information is available free of charge at https://pubs.acs.org/doi/10.1021/acs.inorgchem.9b02724.

Molecular structure of **5**; structural overlay of **1** and $\{Cu(II)[12\text{-MC}_{Cu(II),PicHA}\text{-}4]\}^{2+}$; crystal data, structure refinement, and selected bond lengths and angles for **1**–**5**; protonation constants (logK) of selected compounds; ESI-MS and UV—vis data for Cu(II), Ni(II), and Zn(II) complexes; EPR spectra of Cu(II) complexes (PDF)

Accession Codes

CCDC 1952100-1952104 contain the supplementary crystallographic data for this paper. These data can be obtained free of charge via www.ccdc.cam.ac.uk/data_request/cif, or by emailing data_request@ccdc.cam.ac.uk, or by contacting The Cambridge Crystallographic Data Centre, 12 Union Road, Cambridge CB2 1EZ, UK; fax: +44 1223 336033.

AUTHOR INFORMATION

Corresponding Author

*E-mail: elzbieta.gumienna-kontecka@chem.uni.wroc.pl.

ORCID ®

Igor O. Fritsky: 0000-0002-1092-8035 Vincent L. Pecoraro: 0000-0002-1540-5735

Elzbieta Gumienna-Kontecka: 0000-0002-9556-6378

Notes

The authors declare no competing financial interest.

ACKNOWLEDGMENTS

The project leading to these results has received funding from the European Union's Seventh Framework Programme (FP7/2007-2013) under Marie Skłodowska-Curie grant agreement no. 611488, the Polish National Science Centre (UMO-2017/25/N/ST5/01347), and the U.S. National Science Foundation (CHE 1664964 for V.L.P.).

REFERENCES

- (1) Chakrabarty, R.; Mukherjee, P. S.; Stang, P. J. Supramolecular Coordination: Self-Assembly of Finite Two- and Three-Dimensional Ensembles. *Chem. Rev.* **2011**, *111* (11), 6810–6918.
- (2) Stang, P. J. Abiological Self-Assembly via Coordination: Formation of 2D Metallacycles and 3D Metallacages with Well-Defined Shapes and Sizes and Their Chemistry. *J. Am. Chem. Soc.* **2012**, *134* (29), 11829–11830.
- (3) Hutin, M.; Schalley, C. A.; Bernardinelli, G.; Nitschke, J. R. Helicate, macrocycle, or catenate: Dynamic topological control over subcomponent self-assembly. *Chem. Eur. J.* **2006**, *12* (15), 4069–4076
- (4) Dietrich-Buchecker, C.; Colasson, B. X.; Sauvage, J. P. Molecular knots. *Top. Curr. Chem.* **2005**, 249, 261–283.
- (5) Cook, T. R.; Zheng, Y.-R.; Stang, P. J. Metal-Organic Frameworks and Self-Assembled Supramolecular Coordination Complexes: Comparing and Contrasting the Design, Synthesis, and Functionality of Metal-Organic Materials. *Chem. Rev.* **2013**, *113* (1), 734–777.
- (6) Casini, A.; Woods, B.; Wenzel, M. The Promise of Self-Assembled 3D Supramolecular Coordination Complexes for Biomedical Applications. *Inorg. Chem.* **2017**, *56* (24), 14715–14729.
- (7) Sepehrpour, H.; Fu, W. X.; Sun, Y.; Stang, P. J. Biomedically Relevant Self-Assembled Metallacycles and Metallacages. *J. Am. Chem. Soc.* **2019**, *141* (36), 14005–14020.

(8) Gao, W. X.; Zhang, H. N.; Jin, G. X. Supramolecular catalysis based on discrete heterometallic coordination-driven metallacycles and metallacages. *Coord. Chem. Rev.* **2019**, *386*, 69–84.

- (9) Mezei, G.; Zaleski, C. M.; Pecoraro, V. L. Structural and functional evolution of metallacrowns. *Chem. Rev.* **2007**, *107* (11), 4933–5003.
- (10) Pecoraro, V. L.; Stemmler, A. J.; Gibney, B. R.; Bodwin, J. J.; Wang, H.; Kampf, J. W.; Barwinski, A. Metallacrowns: A new class of molecular recognition agents. *Prog.Inorg. Chem., Vol* 45 **2007**, 45, 83–177
- (11) Lah, M. S.; Pecoraro, V. L. Isolation and characterization of (MnII MnIII(salicylhydroximate) 4(acetate)2(DMF)6).2DMF an inorganic analog of M2+ (12-crown-4). *J. Am. Chem. Soc.* **1989**, *111* (18), 7258–7259.
- (12) Ostrowska, M.; Fritsky, I. O.; Gumienna-Kontecka, E.; Pavlishchuk, A. V. Metallacrown-based compounds: Applications in catalysis, luminescence, molecular magnetism, and adsorption. *Coord. Chem. Rev.* **2016**, 327, 304–332.
- (13) Bodwin, J. J.; Cutland, A. D.; Malkani, R. G.; Pecoraro, V. L. The development of chiral metallacrowns into anion recognition agents and porous materials. *Coord. Chem. Rev.* **2001**, *216*, 489–512.
- (14) Happ, P.; Plenk, C.; Rentschler, E. 12-MC-4 metallacrowns as versatile tools for SMM research. *Coord. Chem. Rev.* **2015**, 289, 238–260.
- (15) Chow, C. Y.; Bolvin, H.; Campbell, V. E.; Guillot, R.; Kampf, J. W.; Wernsdorfer, W.; Gendron, F.; Autschbach, J.; Pecoraro, V. L.; Mallah, T. Assessing the exchange coupling in binuclear lanthanide-(III) complexes and the slow relaxation of the magnetization in the antiferromagnetically coupled Dy-2 derivative. *Chem. Sci.* **2015**, *6* (7), 4148–4159.
- (16) Pavlyukh, Y.; Rentschler, E.; Elmers, H. J.; Hubner, W.; Lefkidis, G. Magnetism of metallacrown single-molecule magnets: From a simplest model to realistic systems. *Phys. Rev. B: Condens. Matter Mater. Phys.* **2018**, *97* (21), 214408.
- (17) Alhassanat, A.; Gamer, I. C.; Rauguth, A.; Athanasopoulou, A. A.; Sutter, J.; Luo, C.; Ryll, H.; Radu, F.; Sapozhnik, A. A.; Mashoff, T.; Rentschler, E.; Elmers, H. J. Element-specific magnetic properties of mixed 3d-4 f metallacrowns. *Phys. Rev. B: Condens. Matter Mater. Phys.* **2018**, 98 (6), No. 064428.
- (18) Athanasopoulou, A. A.; Carrella, L. M.; Rentschler, E. Synthesis, Structural, and Magnetic Characterization of a Mixed 3d/4f 12-Metallacrown-4 Family of Complexes. *Inorganics* **2018**, *6* (3), 66.
- (19) Happ, P.; Rentschler, E. Enforcement of a high-spin ground state for the first 3d heterometallic 12-metallacrown-4 complex. *Dalton Trans.* **2014**, 43 (41), 15308–15312.
- (20) Chow, C. Y.; Guillot, R.; Riviere, E.; Kampf, J. W.; Mallah, T.; Pecoraro, V. L. Synthesis and Magnetic Characterization of Fe(III)-Based 9-Metallacrown-3 Complexes Which Exhibit Magnetorefrigerant Properties. *Inorg. Chem.* **2016**, *55* (20), 10238–10247.
- (21) Boron, T. T., III; Kampf, J. W.; Pecoraro, V. L. A Mixed 3d-4f 14-Metallacrown-5 Complex That Displays Slow Magnetic Relaxation through Geometric Control of Magnetoanisotropy. *Inorg. Chem.* **2010**, 49 (20), 9104–9106.
- (22) Grant, J. T.; Jankolovits, J.; Pecoraro, V. L. Enhanced Guest Affinity and Enantioselectivity through Variation of the Gd3+ 15-Metallacrown-5 Side Chain. *Inorg. Chem.* **2012**, *51* (15), 8034–8041.
- (23) Jankolovits, J.; Lim, C.-S.; Mezei, G.; Kampf, J. W.; Pecoraro, V. L. Influencing the Size and Anion Selectivity of Dimeric Ln(3+) 15-Metallacrown-5 Compartments through Systematic Variation of the Host Side Chains and Central Metal. *Inorg. Chem.* **2012**, *51* (8), 4527–4538.
- (24) Jankolovits, J.; Kampf, J. W.; Maldonado, S.; Pecoraro, V. L. Voltammetric Characterization of Redox-Inactive Guest Binding to Ln(III) 15-Metallacrown-5 Hosts Based on Competition with a Redox Probe. *Chem. Eur. J.* **2010**, *16* (23), 6786–6796.
- (25) Sgarlata, C.; Giuffrida, A.; Trivedi, E. R.; Pecoraro, V. L.; Arena, G. Anion Encapsulation Drives the Formation of Dimeric Gd-III 15-

metallacrown-5 (3+) Complexes in Aqueous Solution. *Inorg. Chem.* **2017**, *56* (9), 4771–4774.

- (26) Trivedi, E. R.; Eliseeva, S. V.; Jankolovits, J.; Olmstead, M. M.; Petoud, S.; Pecoraro, V. L. Highly Emitting Near-Infrared Lanthanide "Encapsulated Sandwich" Metallacrown Complexes with Excitation Shifted Toward Lower Energy. J. Am. Chem. Soc. 2014, 136 (4), 1526–1534.
- (27) Jankolovits, J.; Andolina, C. M.; Kampf, J. W.; Raymond, K. N.; Pecoraro, V. L. Assembly of Near-Infrared Luminescent Lanthanide Host(Host-Guest) Complexes With a Metallacrown Sandwich Motif. *Angew. Chem., Int. Ed.* **2011**, *50* (41), 9660–9664.
- (28) Chow, C. Y.; Eliseeva, S. V.; Trivedi, E. R.; Nguyen, T. N.; Kampf, J. W.; Petoud, S.; Pecoraro, V. L. Ga3+/Ln3+ Metallacrowns: A Promising Family of Highly Luminescent Lanthanide Complexes That Covers Visible and Near-Infrared Domains. *J. Am. Chem. Soc.* **2016**, *138* (15), 5100–5109.
- (29) Rajczak, E.; Pecoraro, V. L.; Juskowiak, B. Sm(III) 12-MCGa(III)shi-4 as a luminescent probe for G-quadruplex structures. *Metallomics* **2017**, *9* (12), 1735–1744.
- (30) Martinic, I.; Eliseeva, S. V.; Nguyen, T. N.; Foucher, F.; Gosset, D.; Westall, F.; Pecoraro, V. L.; Petoud, S. Near-infrared luminescent metallacrowns for combined in vitro cell fixation and counter staining. *Chem. Sci.* **2017**, *8* (9), 6042–6050.
- (31) Martinic, I.; Eliseeva, S. V.; Nguyen, T. N.; Pecoraro, V. L.; Petoud, S. Near-Infrared Optical Imaging of Necrotic Cells by Photostable Lanthanide-Based Metallacrowns. *J. Am. Chem. Soc.* **2017**, 139 (25), 8388–8391.
- (32) Gumienna-Kontecka, E.; Golenya, I. A.; Dudarenko, N. M.; Dobosz, A.; Haukka, M.; Fritsky, I. O.; Swiatek-Kozlowska, J. A new Cu(II) 12 metallocrown-4 pentanuclear complex based on a Cu(II)-malonomonohydroxamic acid unit. *New J. Chem.* **2007**, *31* (10), 1798–1805
- (33) Tegoni, M.; Remelli, M. Metallacrowns of copper(II) and aminohydroxamates: Thermodynamics of self assembly and host-guest equilibria. *Coord. Chem. Rev.* **2012**, 256 (1–2), 289–315.
- (34) Remelli, M.; Bacco, D.; Dallavalle, F.; Lazzari, E.; Marchetti, N.; Tegoni, M. Stoichiometric diversity of Ni(II) metallacrowns with beta-alaninehydroxamic acid in aqueous solution. *Dalton Trans.* **2013**, 42 (22), 8018–8025.
- (35) Bacco, D.; Bertolasi, V.; Dallavalle, F.; Galliera, L.; Marchetti, N.; Marchio, L.; Remelli, M.; Tegoni, M. Metallacrowns of Ni(II) with alpha-aminohydroxamic acids in aqueous solution: beyond a 12-MC-4, an unexpected (vacant?) 15-MC-5. *Dalton Trans.* **2011**, 40 (11), 2491–2501.
- (36) Gumienna-Kontecka, E.; Golenya, I. A.; Szebesczyk, A.; Haukka, M.; Kraemer, R.; Fritsky, I. O. Coordination Diversity in Mono- and Oligonuclear Copper(II) Complexes of Pyridine-2-Hydroxamic and Pyridine-2,6-Dihydroxamic Acids. *Inorg. Chem.* **2013**, 52 (13), 7633–7644.
- (37) Marchio, L.; Marchetti, N.; Atzeri, C.; Borghesani, V.; Remelli, M.; Tegoni, M. The peculiar behavior of Picha in the formation of metallacrown complexes with Cu(II), Ni(II) and Zn(II) in aqueous solution. *Dalton Trans.* **2015**, *44* (7), 3237–3250.
- (38) Wozniczka, M.; Swiatek, M.; Pajak, M.; Gadek-Sobczynska, J.; Chmiela, M.; Gonciarz, W.; Lisiecki, P.; Pasternak, B.; Kufelnicki, A. Complexes in aqueous cobalt(II)-2-picolinehydroxamic acid system: Formation equilibria, DNA-binding ability, antimicrobial and cytotoxic properties. *J. Inorg. Biochem.* **2018**, *187*, 62–72.
- (39) Safyanova, I. S.; Golenya, I. A.; Pavlenko, V. A.; Gumienna-Kontecka, E.; Pekhnyo, V. I.; Bon, V. V.; Fritsky, I. O. Synthesis and Molecular Structures of Cu-II 15-Metallacrown-5 Complexes with Encapsulated Ca-II, Pr-III and Nd-III Ions. *Z. Anorg. Allg. Chem.* **2015**, *641* (12–13), 2326–2332.
- (40) Jankolovits, J.; Kampf, J. W.; Pecoraro, V. L. Isolation of Elusive Tetranuclear and Pentanuclear M(II)-Hydroximate Intermediates in the Assembly of Lanthanide 15-Metallacrown-5 Complexes. *Inorg. Chem.* **2013**, *52* (9), 5063–5076.
- (41) Jankolovits, J.; Kampf, J. W.; Pecoraro, V. L. Insight into the structural versatility of the Ln(III) 15-metallacrown-5 platform by

comparing analogs with Ni(II), Cu(II), and Zn(II) ring ions. *Polyhedron* **2013**, 52, 491–499.

- (42) Golenya, I. A.; Gumienna-Kontecka, E.; Boyko, A. N.; Haukka, M.; Fritsky, I. O. Collapsed Cu(II)-Hydroxamate Metallacrowns. *Inorg. Chem.* **2012**, *51* (11), 6221–6227.
- (43) Seda, S. H.; Janczak, J.; Lisowski, J. Synthesis and structural characterisation of nickel 15-metallacrown-5 complexes with lanthanide(III) and lead(II) ions: Influence of the central metal ion size on the spin state of peripheral nickel(II) ions. *Inorg. Chem. Commun.* **2006**, *9* (8), 792–796.
- (44) Seda, S. H.; Janczak, J.; Lisowski, J. Synthesis and reactivity of copper(II) metallacrowns with (S)-phenylalanine and 2-picolinehydroxamic acids. *Inorg. Chim. Acta* **2006**, 359 (4), 1055–1063.
- (45) CrysAlisRED, Version 1.171.34.76; Oxford Diffraction Ltd., 2003
- (46) Dolomanov, O. V.; Bourhis, L. J.; Gildea, R. J.; Howard, J. A. K.; Puschmann, H. OLEX2: a complete structure solution, refinement and analysis program. *J. Appl. Crystallogr.* **2009**, *42*, 339–341.
- (47) Sheldrick, G. M. SHELXT Integrated space-group and crystal-structure determination. *Acta Crystallogr., Sect. A: Found. Adv.* **2015**, 71, 3–8.
- (48) Gans, P.; O'Sullivan, B. GLEE, a new computer program for glass electrode calibration. *Talanta* **2000**, *51* (1), 33–37.
- (49) Gans, P.; Sabatini, A.; Vacca, A. Superquad an improved general program for computation of formation-constants from potentiometric data. *J. Chem. Soc., Dalton Trans.* **1985**, No. 6, 1195–1200.
- (50) Gans, P.; Sabatini, A.; Vacca, A. HYPERQUAD2006; Protonic Software: Leeds, UK, University of Florence: Florence, Italy.
- (51) Gans, P.; Sabatini, A.; Vacca, A. Investigation of equilibria in solution. Determination of equilibrium constants with the HYPER-QUAD suite of programs. *Talanta* **1996**, *43* (10), 1739–1753.
- (52) Mackellar, W. J.; Rorabacher, D. B. Solvent effects in coordination kinetics 0.1. Inner-sphere effects in reaction of solvated nickel(II) ion with ammonia in methanol-water mixtures. *J. Am. Chem. Soc.* **1971**, 93 (18), 4379–4387.
- (53) Gampp, H.; Maeder, M.; Meyer, C. J.; Zuberbuhler, A. D. Calculation of equilibrium-constants from multiwavelength spectroscopic data. 4. Model-free least-squares refinement by use of evolving factor-analysis. *Talanta* **1986**, 33 (12), 943–951.
- (54) Llunell, M.; Casanova, D.; Cirera, J.; Alemany, P.; Alvarez, S. SHAPE, version 2.1; Universitat de Barcelona, Barcelona, Spain, 2013.
- (55) Addison, A. W.; Rao, T. N.; Reedijk, J.; Vanrijn, J.; Verschoor, G. C. Synthesis, structure, and spectroscopic properties of copper(ii) compounds containing nitrogen sulfur donor ligands the crystal and molecular-structure of aqua 1,7-bis(n-methylbenzimidazol-2'-yl)-2,6-dithiaheptane copper(II) perchlorate. *J. Chem. Soc., Dalton Trans.* 1984, No. 7, 1349–1356.
- (56) Tegoni, M.; Remelli, M.; Bacco, D.; Marchio, L.; Dallavalle, F. Copper(II) 12-metallacrown-4 complexes of alpha, beta- and gamma-aminohydroxamic acids: a comparative thermodynamic study in aqueous solution. *Dalton Trans.* **2008**, No. 20, 2693–2701.
- (57) Seda, S. H.; Janczak, J.; Lisowski, J. Synthesis and structural characterisation of copper(II) 15-metallacrown-5 complexes with Pb-II, Hg-II, Ag-I, Na-I and Y-III central metal ions. *Eur. J. Inorg. Chem.* **2007**, 2007 (19), 3015–3022.
- (58) Johnson, J. A.; Kampf, J. W.; Pecoraro, V. L. The preparation of a double metallahelicate containing 28 copper atoms. *Angew. Chem., Int. Ed.* **2003**, 42 (5), 546–549.
- (59) Stemmler, A. J.; Barwinski, A.; Baldwin, M. J.; Young, V.; Pecoraro, V. L. Facile preparation of face differentiated, chiral 15-metallacrown-5 complexes. *J. Am. Chem. Soc.* **1996**, *118* (47), 11962–11963.
- (60) Zaleski, C. M.; Lim, C.-S.; Cutland-Van Noord, A. D.; Kampf, J. W.; Pecoraro, V. L. Effects of the Central Lanthanide Ion Crystal Radius on the 15-MCCuII(N)pheHA-5 Structure. *Inorg. Chem.* **2011**, 50 (16), 7707–7717.

(61) Cutland, A. D.; Halfen, J. A.; Kampf, J. W.; Pecoraro, V. L. Chiral 15-metallacrown-5 complexes differentially bind carboxylate anions. *J. Am. Chem. Soc.* **2001**, *123* (25), 6211–6212.

- (62) Lim, C. S.; Tegoni, M.; Jakusch, T.; Kampf, J. W.; Pecoraro, V. L. Clarifying the Mechanism of Cation Exchange in Ca(II) 15-MCCu(II)Ligand-5 Complexes. *Inorg. Chem.* **2012**, *51* (21), 11533–11540.
- (63) Schulman, S. G.; Capomacchia, A. C. Dual fluorescence of quinolinium cation. *J. Am. Chem. Soc.* **1973**, 95 (9), 2763–2766.
- (64) Grandberg, I. I.; Faizova, G. K.; Kost, A. N. Comparative basicities of substituted pyridines and electronegativity series for substituents in the pyridine series. *Khim. Geterotsikl. Soedin.* **1966**, 2 (4), 561–566.
- (65) Matsui, H.; Ohtaki, H. A potentiometric study on mixed-ligand cadmium(II) complexes with 2-pyridinecarboxylic acid and 2-aminoalkanoic acids. *Bull. Chem. Soc. Jpn.* **1982**, *55* (7), 2131–2133.
- (66) Anderegg, G. Chelate complexes with methylmercury and phenylmercury cations. *Helv. Chim. Acta* **1974**, *57* (5), 1340–1346.
- (67) Halverson, F.; Hirt, R. C. Near ultraviolet solution spectra of the diazines. *J. Chem. Phys.* **1951**, *19* (6), 711–718.
- (68) Toma, H. E.; Borges, R. H. U. Kinetics and equilibrium studies of iron(II) complexes with pyrazinecarboxylate and 1,10 bipyridyl ligands. *J. Coord. Chem.* **1981**, *11* (3), 143–152.
- (69) Billes, F.; Toth, A. Spectroscopic and calculated ionization-constants of some pyrazines and pyridazines. *J. Chem. Soc., Perkin Trans.* 2 **1986**, No. 3, 359–364.
- (70) Balestrieri, F.; Chiacchierini, E.; Magri, A. L.; Petrone, V. Spectrophotometric investigation on the reaction of indium(III) with methylthymol blue in aqueous acidic medium. *Ann. Chim.* **1978**, *68* (7–8), 525–533.
- (71) Kornreich-Leshem, H.; Ziv, C.; Gumienna-Kontecka, E.; Arad-Yellin, R.; Chen, Y.; Elhabiri, M.; Albrecht-Gary, A. M.; Hadar, Y.; Shanzer, A. Ferrioxamine B analogues: Targeting the FoxA uptake system in the pathogenic Yersinia enterocolitica. *J. Am. Chem. Soc.* **2005**, *127* (4), 1137–1145.
- (72) Dallavalle, F.; Tegoni, M. Speciation and structure of copper(II) complexes with (S)-phenylalanine- and (S)-tryptophanhydroxamic acids in methanol/water solution: a combined potentiometric, spectrophotometric, CD and ESI-MS study. *Polyhedron* **2001**, 20 (21), 2697–2704.
- (73) Pavlishchuk, A. V.; Kolotilov, S. V.; Zeller, M.; Lofland, S. E.; Kiskin, M. A.; Efimov, N. N.; Ugolkova, E. A.; Minin, V. V.; Novotortsev, V. M.; Addison, A. W. Supramolecular Maleate Adducts of Copper(II) 12-Metallacrown-4: Magnetism, EPR, and Alcohol Sorption Properties. *Eur. J. Inorg. Chem.* **2017**, 2017 (41), 4866–4878.
- (74) Kurzak, B.; Kozlowski, H.; Farkas, E. Hydroxamic and aminohydroxamic acids and their complexes with metal-ions. *Coord. Chem. Rev.* **1992**, *114* (2), 169–200.
- (75) Gibney, B. R.; Kessissoglou, D. P.; Kampf, J. W.; Pecoraro, V. L. Copper(II) 12-metallacrown-4 synthesis, structure, ligand variability, and solution dynamics in the 12-MC-4 structural motif. *Inorg. Chem.* **1994**, 33 (22), 4840–4849.
- (76) Lago, A. B.; Pasan, J.; Canadillas-Delgado, L.; Fabelo, O.; Casado, F. J. M.; Julve, M.; Lloret, F.; Ruiz-Perez, C. A three-dimensional copper(II) 12-metallacrown-4 complex with malonomonohydroxamic acid (H(3)mmh) as a ligand. *New J. Chem.* **2011**, 35 (9), 1817–1822.
- (77) Stemmler, A. J.; Kampf, J. W.; Kirk, M. L.; Atasi, B. H.; Pecoraro, V. L. The preparation, characterization, and magnetism of copper 15-metallacrown-5 lanthanide complexes. *Inorg. Chem.* **1999**, 38 (12), 2807–2817.
- (78) Farkas, E.; Szoke, J.; Kiss, T.; Kozlowski, H.; Bal, W. Complex-forming properties of l-alpha-alaninehydroxamic acid (2-amino-n-hydroxypropanamide). *J. Chem. Soc., Dalton Trans.* **1989**, No. 11, 2247–2251.
- (79) Kapinos, L. E.; Sigel, H. Acid-base and metal ion binding properties of pyridine-type ligands in aqueous solution. Effect of ortho

substituents and interrelation between complex stability and ligand basicity. *Inorg. Chim. Acta* **2002**, 337, 131–142.